NIH Public Access
Author Manuscript
Optom Vis Sci. Author manuscript; available in PMC 2011 December 11.

Published in final edited form as:
Optom Vis Sci. 2010 September ; 87(9): 642–655. doi:10.1097/OPX.0b013e3181ea16ea.

Peripheral Refraction with and without Contact Lens Correction

Jie Shen, MD, PhD, **Christopher A. Clark, OD**, **P. Sarita Soni, OD, MS, FAAO**, and **Larry N. Thibos, PhD, FAAO**
School of Optometry, Indiana University, Bloomington, Indiana

Abstract

Purpose—Peripheral refractive error degrades the quality of retinal images and has been hypothesized to be a stimulus for the development of refractive error. The purpose of this study was to investigate the changes in refractive error across the horizontal visual field produced by contact lenses (CLs) and to quantify the effect of CLs on peripheral image blur.

Methods—A commercial Shack-Hartmann aberrometer measured ocular wavefront aberrations in 5° steps across the central 60° of visual field along the horizontal meridian before and after CLs correction. Wavefront refractions for peripheral lines-of-sight were based on the full elliptical pupil encountered in peripheral measurements. Curvature of field is the change in peripheral spherical equivalent relative to the eye's optical axis.

Results—Hyperopic curvature of field in the naked eye increases with increasing amounts central myopic refractive error as predicted by Atchison (2006). For an eccentricity of E degrees, field curvature is approximately E percent of foveal refractive error. Rigid gas permeable (RGP) lenses changed field curvature in the myopic direction twice as much as soft contact lenses (SCLs). Both of these effects varied with CLs power. For all lens powers, SCL cut the degree of hyperopic field curvature in half whereas RGP lenses nearly eliminated field curvature. The benefit of reduced field curvature was partially offset by increased oblique astigmatism. The net reduction of retinal blur due to CLs is approximately constant across the visual field.

Conclusions—Both SCL and RGP lenses reduced the degree of hyperopic field curvature present in myopic eyes, with RGP lenses having greater effect. The tradeoff between field curvature and off-axis astigmatism with RGP lenses may limit their effectiveness for control of myopia progression. These results suggest that axial growth mechanisms that depend on retinal image quality will be affected more by RGP than by SCL lenses.

Keywords

myopia; peripheral refraction; contact lenses; wavefront aberrometry

CONTROL OF EYE GROWTH

Axial myopia is characterized by elongation of the eye's vitreous chamber, resulting in the image of distant objects being focused in front of the retina.[1–4] Animal models show that eye growth is influenced by defocus during the period of emmetropization.[5–8] Optical blur due to hyperopic defocus is thought to provide a stimulus for localized compensatory eye

Corresponding author: Larry N. Thibos, School of Optometry, Indiana University, 800 E. Atwater Ave, Bloomington, IN 47405, thibos@indiana.edu.

Publisher's Disclaimer: This is a PDF file of an unedited manuscript that has been accepted for publication. As a service to our customers we are providing this early version of the manuscript. The manuscript will undergo copyediting, typesetting, and review of the resulting proof before it is published in its final citable form. Please note that during the production process errors may be discovered which could affect the content, and all legal disclaimers that apply to the journal pertain.

NIH-PA Author Manuscript
NIH-PA Author Manuscript
NIH-PA Author Manuscript

NIH-PA Author Manuscript

NIH-PA Author Manuscript

NIH-PA Author Manuscript

elongation[9] to realign the retina with the image location.[10] Support for this hypothesis has been garnered from animal experiments in birds[11, 12] and several mammal models[13, 14] including primates.[15, 16] but contrary evidence has also been reported.[17]

Animal studies have further demonstrated that ocular growth is controlled by local retinal mechanisms[18–21] that act to minimize image degradation at the corresponding retinal location by changing axial eye growth rate over a restricted area.[21] For example, animals that consistently experience near objects in their inferior visual field have longer ocular length in the upper half of the globe.[22, 23] Similarly, Seidemann and colleagues[24] found more myopia in the inferior visual field than the superior visual field in a group of human emmetropes. In recent studies performed using infant monkeys, optically imposed hyperopic defocus in the periphery or selective peripheral form deprivation can produce central axial myopia.[25–27] These studies suggested that visual signals from the periphery can dominate the overall axial growth of the eye.

Compelling evidence of the potential role of peripheral vision in human myopia progression emerged from two recent longitudinal studies demonstrating that orthokeratology lenses reduce the progression of childhood myopia.[28, 29] Both studies reported that vitreous chamber depth (VCD) grew significantly less in ortho-k treated children compared with children who have traditional vision correction.

Peripheral Refraction and Myopia Progression

Multiple studies[24, 30–32] have shown that hyperopic and emmetropic eyes tend to have peripheral refractive errors that are myopic relative to the fovea. Figure 1A illustrates a typical case of emmetropic eyes: rays from a distant fixation point are focused on the retina but rays from distant objects in the peripheral field are focused in front of the retina. The image shell from a distant, extended object is therefore more curved than the retinal surface, resulting in an increasing amount of myopic blur at greater retinal eccentricities. In this paper, we will refer to this condition as “myopic field curvature” or “relative peripheral myopia”. By contrast, myopic eyes tend to have less myopia in the peripheral visual field than foveally. Most authors agree on this point for the horizontal field, but there is some controversy regarding the generality of the finding to other meridia.[24, 33, 34] As shown in Fig. 1B, the image shell from a distant, extended object is less curved than the retinal surface in myopic eyes, resulting in a decreasing amount of myopic blur at greater retinal eccentricities. Thus, relative to foveal refractive error, the eye has an increasing amount of hyperopic blur at greater retinal eccentricities. In this paper, we will refer to this condition as “hyperopic field curvature” or “relative peripheral hyperopia”.

Evidence suggests that hyperopic field curvature is associated with myopia progression in human eyes.[35–37] For example, young pilots with hyperopic field curvature were more likely to develop adult-onset myopia than those who showed myopic field curvature in at least in one meridian[35] In a large scale study of school children, eyes that became myopic experienced accelerated growth prior to onset that converted myopic field curvature into hyperopic field curvature.[38] Although this reversal in sign of field curvature may have been secondary to some other factor driving ocular growth initially, it may nevertheless have exacerbated the progression of myopia. This hypothesis is supported by the work of Smith and colleagues[26] who tested the hypothesis that peripheral visual experience contributes to ocular growth and central refractive development in primates. Their study provided strong evidence that peripheral retinal mechanism can influence the refractive development at the fovea.

In the human fovea, the diameter of the rod free area (where spatial vision is most acute) is approximately 1°,[39] which is less than 1% of the diameter of the visual field. Thus the area

NIH-PA Author Manuscript

NIH-PA Author Manuscript

NIH-PA Author Manuscript

of retina devoted to high spatial resolution that is assessed during subjective measurements of refractive error is 4 orders of magnitude smaller than the surrounding retinal area. Given this huge imbalance, it would not be surprising if peripheral refractive errors dominate the development of refractive error.[20] Even if local mechanisms were to sense a difference between foveal and peripheral refractive errors, mechanical constraints are likely to force the fovea to elongate axially in accordance with the surrounding, peripheral retina.

Contact Lenses and Myopia Progression

Soft and rigid contact lenses are widely used treatments for refractive errors. Although lenses are prescribed to correct central vision, they affect the peripheral field as well and therefore may influence eye growth globally. Studies of the effects of soft contact lenses on the progression of myopia have reported no effect on refractive development[40, 41] or small but clinically insignificant effects.[42] Studies using rigid contact lenses have reported slowing of myopia progression[43, 44] or no effect[45] or an increase the progression of myopia.[46] The recent CLAMP (Contact Lens and Myopia Progression) study found that RGP lenses reduced the rate of progression of myopia in children, but this was largely due to flattening of the cornea rather than slowing of axial elongation.[47] None of these studies considered the effect of the lenses on peripheral refractive errors or their contribution to myopia progression.

Given the potential effect of peripheral image blur on the development of central refractive error described above, we investigated the effect of contact lenses on the refractive status of the peripheral visual field. As illustrated in Fig. 1C, the contact lens may exaggerate, maintain, neutralize, or reverse the curvature of field in the myopic eye. For example, if the contact lens adds the same dioptric power to peripheral lines-of-sight as it does to the foveal line-of-sight, then the curvature of field will be unaffected. In this case we would predict that the peripheral relative hyperopia will continue to promote progression of myopia (image shell #3). If the eye's curvature of field is completely corrected by the contact lens (image shell #2) or the contact lens could reverse the sign of the peripheral relative error thereby converting hyperopic field curvature into myopic field curvature (image shell #1), then the stimulus to eye growth will be eliminated and that would presumably slow the progression of myopia.[20, 24]

Given the various possible outcomes of contact lens treatment on peripheral refractive error, and the potential significance of that refractive error on myopia progression, we aimed to experimentally measure the changes in sphero-cylindrical refraction across the visual field produced by soft and rigid contact lenses. Although the peripheral aberrations of contact lenses in isolation have been reported previously,[48] to obtain a definitive result of how the peripheral refractive error and image quality changes across the visual field due to contact lens correction requires that the lenses be worn by a human eye. This was the purpose of our study.

METHODS

Subjects

This study followed the tenets of the Declaration of Helsinki. Informed consent was acquired from all subjects following approval by the Indiana University institutional review board. Optical modeling indicated that the effect of contact lenses on field curvature will depend on lens power. Therefore, to obtain a comprehensive assessment we chose to study eyes with a range of refractive errors. Eleven young normal subjects (5 female and 6 males, 23~30 yrs) with myopia from −1 to −6.5 D were included initially, but two were eliminated for reasons stated below, leaving a total of 9 subjects for whom data are presented in this

NIH-PA Author Manuscript

NIH-PA Author Manuscript

NIH-PA Author Manuscript

report. None of the subjects had astigmatism greater than 2 D. The inclusion criteria included best corrected logMAR visual acuity of 0.00 (20/20 Snellen acuity) or better in both eyes. In addition, subjects were expected to have stable refractive error in the past 12 months and to be free of any ocular or systemic disease or medications. No cycloplegic drugs were used.

Instruments

Refraction measurements were obtained with a COAS wavefront aberrometer (Wavefront Science, Inc.) on the subject's left eye in a dark room to ensure the largest pupil size. We chose this instrument, rather than a conventional optometer, because it uses a Shack-Hartmann (SH) wavefront sensor to obtain a detailed wavefront analysis of the entire entrance pupil, even when the pupil appears elliptical when viewed obliquely. According to the manufacturer's specifications, the COAS can measure spherical refractive errors within the range of −15.00 to +7.00 D with an accuracy of ±0.10 D and a repeatability of ±0.05 D. Subjects were aligned with the aberrometer using internal cameras of COAS that are co-axial with the wavefront sensor and are focused using the virtual Purkinje images of light-emitting diodes on the face of the instrument. Validation studies have shown that results obtained from the COAS aberrometer are robust against small misalignments that might occur for off-axis measurements.[49] The COAS aberrometer has been shown to be a valid instrument for measuring peripheral ocular aberrations for elliptical entrance pupils that occur off axis.[50] The range of field angles for which valid measurements are obtainable may differ from subject to subject. Our criterion for data integrity was the complete filling of the entrance pupil with SH spots in the aberrometer's data image. The pupil diameter in the horizontal and vertical directions was measured by counting spots in the SH data image. These values were compared with dimensions obtained from images of the entrance pupil obtained independently by the COAS iris camera that served as a pupilometer. Additional methodological details are documented elsewhere.[50]

There are two ways to acquire off-axis measurements of ocular aberrations. One method (eye rotation) uses a fixation target in the peripheral visual field to elicit eye rotation (keeping head fixed) relative to the aberrometer's measurement axis. Another way (head rotation) is to keep the eye in the primary position of gaze but rotate the head with respect to the measurement axis. A previous study has shown that measurements by these two are the same for central and peripheral refraction in the naked eye.[51] We anticipated that in our experiments the alignment of the contact lens to the eye will change if the eye rotates, and therefore we chose the head rotation method. This was achieved by modifying the chin rest to rotate around a vertical axis. Rotation angles were quantified in 5° steps up to 45° temporally and nasally. A fixation target was attached to a support bracket of the chin rest assembly so that eye position relative to the head remained fixed as the head rotated. In the 0° position, the fixation target coincided with the laser probe beam of the aberrometer. The fixation target was visible to subjects through a beam splitter (Figure 2). The vergence of the target was adjustable so that the subject's accommodation was relaxed by setting the target to the subject's far point. Subjects were instructed to fixate on the visual target during the experiment. For comfort the subject's body rotated as the head rotated with the chin rest rotation.

Contact Lenses

We used Acuvue 2 (base curve: 8.3mm, overall diameter (OAD): 14mm) and Menicon RGP (OAD: 9.2mm, optic zone: 7.8mm, Menicon Z matieral with Dk (ISO) = 163) lenses. The RGP lenses had the same design and lens parameters as those used in the CLAMP study.[47] The alignment fitting strategy (fluorescein pattern shows alignment of back surface of the

NIH-PA Author Manuscript

NIH-PA Author Manuscript

NIH-PA Author Manuscript

lens with the cornea over most of the surface)[52] based on individual eye's ketratometry readings was used in all of our subjects (base curve: 7.67 ± 0.26 mm).

Data Collecting and Analysis

Three measurements were taken at each visual eccentricity, with realignment of the eye to the instrument between measurements. Subjects blinked before measurements to ensure tear film integrity. Measurements were taken after the contact lens stabilized on the eye between blinks. In our previous paper,[50] we demonstrated the validity of using commercial software CLAS-2D to analyze off-axis data. The software allows users to draw an analysis Zernike circle that is concentric with, and surrounds, the elliptical entrance pupil. Computation of the Zernike coefficients ignores the area between the Zernike analysis circle and the elliptical entrance pupil. Mean pupil diameter across all subjects was 6.89 mm and the largest pupil was 7.2 mm. We therefore used a 7.2 mm circle as a common basis for Zernike analysis of all eyes. Having determined the Zernike coefficients, we computed the eye's sphero-cylindrical refractive error from 2nd order terms. All results refer to 840 nm wavelength infrared laser light which was used in COAS aberrometer. No correction for ocular chromatic aberration was required for differential results that quantify relative changes. Power vector notation[53] (M: the spherical equivalent, J_0: with-the-rule (WTR) and against-the-rule (ATR) astigmatism, J_{45}: oblique astigmatism with axes at 45 deg and 135 deg) was used to indicate the optimum correcting lens for each line-of-sight (peripheral and foveal). The relationship between 2nd order Zernike coefficients and sphero-cylindrical components M, J_0, J_{45} is given by the following equations.[54]

$$\begin{aligned} M &= \frac{-4\sqrt{3}}{r^2} C_2^0 \\ J_0 &= \frac{-2\sqrt{6}}{r^2} C_2^2 \\ J_{45} &= \frac{-2\sqrt{6}}{r^2} C_2^{-2} \end{aligned} \quad (1)$$

Where C_2^0, C_2^2, C_2^{-2} are Zernike coefficients for defocus, WTR/ATR astigmatism and oblique astigmatism terms, and *r* is pupil radius. For convenience we will refer to the change in spherical equivalent refractive error with eccentricity as "peripheral relative M" (PRM). Similarly, changes in the astigmatic components are called "peripheral relative J_0" (PRJ_0) and "peripheral relative J_{45}" (PRJ_{45}).

Reference Axis and Optical Modeling

The nasal-temporal asymmetry of refractive error evident in the literature[31, 55–57] is thought to be due to angle alpha between the visual axis and the eye's optical axis.[58, 59] Therefore, to achieve a clearer understanding of the eye's optical properties across the visual field, curvature of field and peripheral astigmatism are referenced to the optical axis rather than the foveal line-of-sight. To make this adjustment we assumed the optical axis is 5° temporal from the foveal line-of-sight, which removed the nasal/temporal asymmetry.

The computer program Visual Optics Laboratory (VOL-Pro, version 7.30, Sarver & Associates, Inc., Carbondale, Illinois) was used to predict the curvature of field and peripheral astigmatism to be expected in a typical human eye. For this purpose we used Atchison's myopic model eye[60] with refraction-dependent parameters as the optical model.

NIH-PA Author Manuscript

NIH-PA Author Manuscript

NIH-PA Author Manuscript

RESULTS

The Range of Eccentricities Accessible in Human Subjects

The COAS aberrometer is a double-pass aberrometer based on a Shack-Hartmann wavefront sensor with a limited dynamic range set by an internal range-limiting aperture. As the measurement axis goes further into the peripheral visual field, we anticipated that large amounts of oblique astigmatism, coma, and other higher-order aberrations on both the forward and reverse passes of light could affect our measurement of defocus (i.e. curvature of field). If the highly aberrated rays are blocked by the internal aperture, then spots will be missing from the SH data image which can lead to errors in pupillometry as well as aberrometry. Therefore it was important to conduct an initial experiment to determine the range of eccentricities for which valid data could be obtained over the entire entrance pupil.

Figure 3 shows how the pupil aspect ratio, as measured by counting spots in the aberrometer's data image along the vertical and horizontal meridia, varies with eccentricity across the visual field. In theory, the pupil aspect ratio should vary as the cosine of eccentricity (the broken line with triangle symbol) but in practice the measured value can have an uncertainty equal to the diameter of the lenslets used to create the spots. If a lenslet happens to fall on the edge of the entrance pupil, the spot will be dimmer than the others, and possibly distorted. If these partial spots are included, the pupil diameter will be over-estimated but if omitted the pupil diameter will be under-estimated. Thus a gray band centered on the theoretical curve represents a confidence interval for the theoretical expectation. Most of the experimental data fell within this confidence interval for eccentricities up to ±30°. This means the wavefront sensor measured the entire entrance pupil for most of the subjects for this range of eccentricities. For two subjects the pupil aspect ratio was considerably less than expected across most of the visual field so they were excluded from the following analysis. For the remaining 9 subjects, we excluded data from subsequent analysis when the pupil aspect ratio fell outside the gray band in Fig. 3.

Curvature of Field for the Naked Eye

Previous studies have shown that peripheral spherical refraction varies widely between subjects.[61, 62] Others have suggested that this individual variation in field curvature is due to individual differences in ocular shape combined with other optical features of the myopic eye.[6063, 64] To obtain a quantitative estimate of this effect to guide the interpretation of our experimental results, we used Atchison's myopic model eye[60] to compute the change in peripheral relative refractive error (PRM). The model indicated, for example, that PRM at 15° eccentricity from the eye's optical axis should increase linearly at the rate of 0.06 diopters per diopter of central M in the naked eye. This expected dependence of PRM on foveal refractive error is reflected qualitatively in the data for our 9 subjects shown in Fig. 4. Eyes with low amounts of myopia had relatively weak curvature of field whereas the eyes with large amounts of myopia had strong field curvature. Since PRM increased in the positive direction for off-axis viewing, these naked myopic eyes exhibited hyperopic field curvature.

Figure 5 draws a quantitative comparison between theoretical optical predictions and our experimental data for two individual eyes (−2D and −6.5D myopia). Software restrictions in the current version of VOL limited theoretical modeling to 16° of eccentricity. Nevertheless, the experimental data agree closely with theoretical predictions of field curvature within individual eyes and confirm that greater field curvature occurs in eyes with greater degree of myopia. Further evidence of the strong correlation between the magnitude of field curvature and central refractive error is given in Fig. 6 which includes data from all eyes in the study population, tested at 15° nasal and temporal eccentricity. As central myopic refractive error

NIH-PA Author Manuscript

NIH-PA Author Manuscript

NIH-PA Author Manuscript

increases, field curvature becomes more hyperopic at the rate of approximately 0.06D per diopter of central M. Data from greater eccentricities showed the same trend as in Fig. 6, but with greater slopes.

The heterogeneity of the study population, which by design included eyes covering a range of foveal refractive errors, precludes simple averaging of results in Fig. 4 across subjects. Since the magnitude of field curvature varies in proportion to foveal refractive error, the appropriate statistical treatment is to normalize PRM by foveal refractive error. The result is "normalized field curvature" expressed as a fraction of foveal refractive error. Once normalized, the population becomes homogeneous thereby enabling the meaningful computation of a population mean, shown in Fig. 7. With the exception of measurements at 10° in the temporal visual field relative to optical axis, which we believe are abnormal because of the optic nerve head, the mean data show a monotonic increase in PRM with eccentricity that is approximately linear with a slope of 0.01 diopters/deg of eccentricity. Thus for an eccentricity of E degrees, PRM is approximately E percent of foveal refractive error in the naked eye.

Effect of Contact Lenses on Field Curvature

Measurements of PRM when the eye is corrected by soft or rigid contact lenses are compared with measurements from the naked eye in Fig. 4 for all 9 subjects. Compared to the naked eye, curvature of field was reduced, and in some cases reversed in sign, by contact lenses. To better reveal this effect, Fig. 8 directly compares field curvature at the largest eccentricity measured (beyond 25° relative to optical axis) with and without contact lenses. If contact lenses had no effect on PRM, then the data would lie on the 1:1 line in the graph. To the contrary, most of the data points fall below the line, indicating that, for most eyes, the peripheral relative hyperopia of the naked eye was reduced by the contact lens. This reduction in hyperopic field curvature was greater for the RGP lenses than for the SCLs. Many of the data point in Fig. 8B fall in the $y < 0$ quadrant of the graph, indicating that field curvature changed from hyperopic to myopic as a result of wearing the RGP lens. For most eyes, the variability in repeated measurements was greater with CLs than for the naked eye. This might be due to changes in tear film integrity or contact lens movement after fitting with contact lenses.

The population means of normalized PRM values shown in Fig. 7 confirm that SCLs cut the degree of hyperopic field curvature in half and that RGPs come close to eliminating field curvature. These differences exceed the confidence intervals most clearly at the larger eccentricities. The ordinal ranking of mean PRM values as naked eye (largest), SCL (intermediate), and RGP (smallest) across eccentricities is confirmed by the non-parametric sign test ($p = 0.02$).[65]

The predictive power of Atchison's model of the myopic eye described above for the naked eye suggested a similar modeling of eyes corrected by contact lenses to account for the correlation between PRM of the naked eye and corrected eye shown in Fig. 8. One possible reason for this correlation might be that PRM is correlated with central refractive error (Fig. 6) and eyes with larger central refractive error require a stronger contact lens. A stronger contact lens, in turn, might have a larger curvature of field itself, and therefore would have a larger effect on the measured curvature of field for (eye + lens). To evaluate these ideas, we modeled the case of RGP correction for which the effects are largest and conformation of the lens to the corneal surface can be ignored. The results indicated that correcting the foveal refractive error with a rigid contact lens maintains the linear relationship between PRM and central M, but reduces the rate of PRM increase to 0.04 diopters per diopter of central M (compared to 0.06 diopters per diopter of central M for the naked eye) in 15° periphery (theoretical prediction lines in Fig.6).

NIH-PA Author Manuscript

NIH-PA Author Manuscript

NIH-PA Author Manuscript

Experimental evidence supports the theoretical predictions as shown in Fig. 9, which displays the correlation between contact lens power and the effect of contact lenses on field curvature measured beyond 25° eccentricity. With increasing lens power, both SCLs and RGP lenses showed an increasing effect on PRM. This effect was more than triple for RGP lenses compared to SCLs as indicated by their respective regression slopes (0.14D vs. 0.04D of field curvature change per diopter of lens power). That is, changes in PRM in the myopic direction for RGP lenses was triple that for SCLs of the same power.

Contact Lens Effect on Peripheral Astigmatism

Average value of J_0 (90/180° astigmatism) for the foveal line-of-sight in our subjects was +0.15D, indicating WTR astigmatism that is typical of human eyes.[24, 56] For peripheral lines-of-sight, J_0 decreased with eccentricity up to 10 degree in nasal visual field and 25 degree in temporal visual field as shown in Fig. 10. Eventually J_0 changed sign, indicating ATR astigmatism for larger eccentricities. This behavior is consistent with other experimental studies[31, 56] and theoretical modeling (Figure 10A).[66, 67] The nasal-temporal asymmetry of J_0 evident in Fig. 10A was removed by referencing visual field to the eye's optical axis as shown in Fig. 10B.

The effect of contact lenses on peripheral relative astigmatism is shown in Fig. 11. Not evident in the figure (because peripheral astigmatism is shown relative to axial astigmatism) is the fact that RGP lenses decreased axial astigmatism ($p<.05$, paired t-test) presumably because of the tear film lens formed between the lens and the corneal surface. Starting from 10° relative to eye's optical axis, PRJ_0 increased with RGP correction. SCLs also showed increased astigmatism but with smaller effect than RGP lens (Figure 11A). Compared to PRJ_0, the variation in PRJ_{45} across the horizontal visual field was small (<0.1 D) in naked eyes (Figure 11B) and statistically insignificant. Neither RGP lenses nor SCLs affected PRJ_{45} which was nearly constant over the horizontal visual field.

Contact Lens Effect on Total Sphero-Cylindrical Blur

The results described above show that defocus (M) and astigmatism (J_0) both vary across the visual field. If image quality is a driving force for myopia progression as suggested previously,[68–72] then it is important to determine the combined effects of M and J_0. The effect of contact lenses may be complex because, as shown above, relative hyperopic defocus is reduced by contact lenses, but peripheral astigmatism increases. Therefore, to determine the effect of contact lenses on peripheral image quality, we need to quantify and compare the total sphero-cylindrical image blur on the peripheral retina before and after wearing contact lenses.

If the refractive error for foveal vision is represented by the power vector P and the refractive error for peripheral vision is represented by the power vector P', then the difference P'−P is a vectorial representation of the peripheral relative refractive error. The length of this difference vector quantifies the residual blur on the peripheral retina when viewing through a lens appropriate for central vision. We refer to the length of the difference vector as peripheral relative blur (PRblur) which is calculated by equation 2.

$$PRblur=|P'-P|\sqrt{(M'-M)^2+(J_0'-J_0)^2+(J_{45}'-J_{45})^2} \quad (2)$$

As shown in Fig. 12, the average PRBlur in naked eye increased to 2 D at 35° periphery relative to the eye's optical axis. SCLs did not have a consistent effect on PRblur but RGP lenses consistently reduced PRblur across the visual field ($p < 0.01$, non-parametric sign test) by approximately 0.25 diopter.

NIH-PA Author Manuscript

NIH-PA Author Manuscript

NIH-PA Author Manuscript

DISCUSSION

Our assessment of the refractive state of the naked eye across the horizontal visual field confirms a previous study[33] showing that curvature of field depends on central refractive error. Highly myopic eyes tend to have stronger hyperopic field curvature (i.e. more peripheral relative hyperopia) compared to slightly myopic eyes. This result suggests high myopic eyes have a more prolate shape (longer axial length than equatorial diameter). Several studies have measured ocular parameters physically and confirmed that eye shape becomes more elongated with increasing severity of myopia.[73, 74] Those results and others[24, 30–32] are summarized by an optical model (Fig. 1B) in which the image shell is closer to the retina peripherally than it is centrally. Since eyes typically have off-axis astigmatism, the image shell we are referring to lies at the midpoint of Sturm's interval. When fitted with a contact lens prescribed to correct central refractive error, various outcomes are possible (Fig. 1C). If the CLs add a constant power for all lines-of-sight, there would be no change in the hyperopic curvature of field (image shell #0, Fig. 13 A & B). A lens that fully neutralizes field curvature produces an image shell which perfectly superimposes on the retina both centrally and peripherally. Neither of those predictions was confirmed experimentally. Instead, the results of our study indicated that SCLs partially correct the eye's hyperopic field curvature (Fig. 13 A, image shell #1), and RGP lens correction over corrects field curvature, resulting in myopic field curvature in some cases (Fig. 13B, image shell #2). Note that the image shells shown on Fig. 13 are for illustrative purposes only and were not calculated from experimental data.

We presume the effects of RGP lenses on peripheral refraction will depend on lens design. For example, different design concepts of the RGP lenses might produce different image shells in the corrected eye. Also, various fitting strategies (e.g. on-K, steep or flat fittings) may have different effects on field curvature after CLs correction. Thus, the results reported in this study only refer to the alignment fitting strategy (which is the most commonly used RGP fitting strategy) and the Menicon Z xt design. Further work will be required to determine if differences in peripheral refraction are caused by differently designed RGP lenses or different fitting strategies.

Bennett and Rabbetts pointed out that the overall action of the RGP lens was towards a relatively more positive power[75] in the periphery compared to the center. This indicated that by RGP correction, the peripheral image shell would shift in the myopic direction relative to central. Atchison demonstrated in his eye model that spherical contact lenses produce a myopic shift into periphery and increased J_0 slightly.[60] The results of our VOL modeling based on Atchison's myopic model eye shown in Fig. 14 confirm these prior theoretical conclusions. For illustrative purposes we chose to analyze the paraxial behavior of −3 D myopic eye model with 3.2mm pupil diameter for 0–16° range of eccentricity. A −3 D RGP lens with spherical front and back surface design was used to build our VOL model (modeling SCLs would be more difficult because soft lens conform to the front corneal surface, making it difficult to know how the soft lens will change its shape on the eye). The purpose of the modeling was to show qualitative trends to be expected rather than quantitative predictions of the experimental data. Although a variety of factors preclude close quantitative predictions (e.g. paraxial model vs. large-pupil human eyes, individual variation in corneal curvatures and other model parameters, alignment of the CL to the eye, etc.), the model confirmed the expected trend of how contact lenses affect peripheral refraction on the horizontal meridian. The hyperopic peripheral image shell shifts in the myopic direction, J_0 increases but J_{45} is unaffected, and peripheral relative blur declines. These theoretical calculations are thus qualitatively consistent with the direction of our experimental findings, if not their magnitude. The population mean data show that RGP lenses reduce field curvature but increase off-axis astigmatism with a net reduction of

NIH-PA Author Manuscript

NIH-PA Author Manuscript

NIH-PA Author Manuscript

overall blur (Fig. 12). The theoretical modeling indicates a larger expected benefit, at least paraxially, which suggests the need for refined modeling in future work not only for RGP but also for soft contact lenses.

Peripheral astigmatism increased considerably with off-axis eccentricities[66] in the naked eye. Results from our study and previous theoretical modeling[60] show that RGP lenses actually increased peripheral ATR/WTR astigmatism. Artal et al. suggested that the human eye is an example of robust optical design and corneal aberrations are compensated by the internal optics.[76, 77] Contact lenses may upset this balance between the cornea and internal optics, leaving the whole eye's oblique astigmatism increased. Although earlier studies suggested that astigmatism could influence the development of myopia[78, 79] or emmetropization process,[72] a number of chicken studies suggested that imposed astigmatic error does not play an important role during emmetropization.[80–82] Thus, it is still unclear whether off-axis astigmatism influences refractive error development or not.

As noted above, both the formation of peripheral image shell and peripheral image blur may play important role in refractive error development.[16, 26, 28, 29, 35–38, 68–72] We found that SCLs make the relative hyperopic periphery less hyperopic in myopic eyes, but the peripheral image shell remains relative hyperopic. In addition, SCLs do not have a significant effect on peripheral image blur. This might be one of the reasons that SCLs fail to slow myopia progression as reported in previous studies.[40–42] To the contrary, RGP lenses come close to eliminating field curvature across the visual field and also decrease peripheral image blur. Based on the "grow to compensate hyperopic defocus" or "grow to clarity" hypothesis, RGP lenses are more likely than SCLs to slow myopia progression due to its peripheral optical performance. The increased levels of off-axis astigmatism induced by RGP lenses may or may not influence myopia progression. While image quality certainly suffers from astigmatic blur, animal experiments have shown that means spherical equivalent is more important than total blur in determining eye growth in chicks.[80,83]

In conclusion, both SCL and RGP lenses reduce the degree of hyperopic field curvature present in myopic eyes, but only RGPs reduce the relative amount of image blur on the peripheral retina. Although our study was motivated by the myopia question, the results pertain also to the perceptual quality of peripheral vision. The visual benefit of improved image contrast for peripheral vision obtained by RGP lenses should outweigh the visual benefit of SCLs. The tradeoff between reduced field curvature but increased peripheral astigmatism with RGP correction limits the net improvement of image blur on the peripheral retina that might, in turn, limit RGP lens effectiveness for improving vision or controlling myopia progression. Our results suggest that axial growth mechanisms that depend on retinal image quality will be affected more by RGP than by SCL lenses. These results provide some guidance for future designs of contact lenses to control myopia progression.

Acknowledgments

This work was supported by NIH grant R01-EY05109 and Vistakon Division, Johnson & Johnson Vision Care, Inc. We thank Menicon Co. Ltd. for provide RGP lenses used in this study. We also thank Wavefront Sciences and Sarver & Associates, Inc. for access to their analysis software CLAS-2D and VOL-Pro, respectively. Equipment development was supported by NEI-P30EY019008 "Core Grant for Vision Science".

REFERENCES

1. Carney LG, Mainstone JC, Henderson BA. Corneal topography and myopia. A cross-sectional study. Invest Ophthalmol Vis Sci. 1997; 38:311–320. [PubMed: 9040463]

NIH-PA Author Manuscript

NIH-PA Author Manuscript

NIH-PA Author Manuscript

2. Cheng HM, Singh OS, Kwong KK, Xiong J, Woods BT, Brady TJ. Shape of the myopic eye as seen with high-resolution magnetic resonance imaging. Optom Vis Sci. 1992; 69:698–701. [PubMed: 1437010]

3. Grosvenor T, Scott R. Role of the axial length/corneal radius ratio in determining the refractive state of the eye. Optom Vis Sci. 1994; 71:573–579. [PubMed: 7816428]

4. Llorente L, Barbero S, Cano D, Dorronsoro C, Marcos S. Myopic versus hyperopic eyes: axial length, corneal shape and optical aberrations. J Vis. 2004; 4:288–298. [PubMed: 15134476]

5. Wildsoet CF. Active emmetropization—evidence for its existence and ramifications for clinical practice. Ophthalmic Physiol Opt. 1997; 17:279–290. [PubMed: 9390372]

6. Lu F, Zhou X, Jiang L, Fu Y, Lai X, Xie R, Qu J. Axial myopia induced by hyperopic defocus in guinea pigs: A detailed assessment on susceptibility and recovery. Exp Eye Res. 2009; 89:101–108. [PubMed: 19268468]

7. Wildsoet C, Wallman J. Choroidal and scleral mechanisms of compensation for spectacle lenses in chicks. Vision Res. 1995; 35:1175–1194. [PubMed: 7610579]

8. Smith EL 3rd, Hung LF, Harwerth RS. Effects of optically induced blur on the refractive status of young monkeys. Vision Res. 1994; 34:293–301. [PubMed: 8160365]

9. Wallman J, Gottlieb MD, Rajaram V, Fugate-Wentzek LA. Local retinal regions control local eye growth and myopia. Science. 1987; 237:73–77. [PubMed: 3603011]

10. Wallman J, Adams JI. Developmental aspects of experimental myopia in chicks: susceptibility, recovery and relation to emmetropization. Vision Res. 1987; 27:1139–1163. [PubMed: 3660666]

11. Irving EL, Callender MG, Sivak JG. Inducing myopia, hyperopia, and astigmatism in chicks. Optom Vis Sci. 1991; 68:364–368. [PubMed: 1852398]

12. Schaeffel F, Howland HC. Properties of the feedback loops controlling eye growth and refractive state in the chicken. Vision Res. 1991; 31:717–734. [PubMed: 1843772]

13. Graham B, Judge SJ. The effects of spectacle wear in infancy on eye growth and refractive error in the marmoset (Callithrix jacchus). Vision Res. 1999; 39:189–206. [PubMed: 10326130]

14. Siegwart JT Jr, Norton TT. Regulation of the mechanical properties of tree shrew sclera by the visual environment. Vision Res. 1999; 39:387–407. [PubMed: 10326144]

15. Hung LF, Crawford ML, Smith EL 3rd. Spectacle lenses alter eye growth and the refractive status of young monkeys. Nat Med. 1995; 1:761–765. [PubMed: 7585177]

16. Smith EL 3rd, Huang J, Hung LF, Blasdel TL, Humbird TL, Bockhorst KH. Hemiretinal form deprivation: evidence for local control of eye growth and refractive development in infant monkeys. Invest Ophthalmol Vis Sci. 2009; 50:5057–5069. [PubMed: 19494197]

17. Weizhong L, Zhikuan Y, Wen L, Xiang C, Jian G. A longitudinal study on the relationship between myopia development and near accommodation lag in myopic children. Ophthalmic Physiol Opt. 2008; 28:57–61. [PubMed: 18201336]

18. Diether S, Schaeffel F. Local changes in eye growth induced by imposed local refractive error despite active accommodation. Vision Res. 1997; 37:659–668. [PubMed: 9156210]

19. Hodos W, Kuenzel WJ. Retinal-image degradation produces ocular enlargement in chicks. Invest Ophthalmol Vis Sci. 1984; 25:652–659. [PubMed: 6724835]

20. Wallman J, Winawer J. Homeostasis of eye growth and the question of myopia. Neuron. 2004; 43:447–468. [PubMed: 15312645]

21. Bartmann M, Schaeffel F. A simple mechanism for emmetropization without cues from accommodation or colour. Vision Res. 1994; 34:873–876. [PubMed: 8160400]

22. Fitzke FW, Hayes BP, Hodos W, Holden AL, Low JC. Refractive sectors in the visual field of the pigeon eye. J Physiol. 1985; 369:33–44. [PubMed: 4093886]

23. Hodos W, Erichsen JT. Lower-field myopia in birds: an adaptation that keeps the ground in focus. Vision Res. 1990; 30:653–657. [PubMed: 2378058]

24. Seidemann A, Schaeffel F, Guirao A, Lopez-Gil N, Artal P. Peripheral refractive errors in myopic, emmetropic, and hyperopic young subjects. J Opt Soc Am (A). 2002; 19:2363–2373.

25. Smith EL 3rd, Hung L-F, Ramamirtham R, Huang J, Qiao-Grider Y. Optically imposed hyperopic defocus in the periphery can produce central axial myopia in infant monkeys. Invest Ophthalmol Vis Sci. 2007; 48 E-Abstract 1533.

NIH-PA Author Manuscript

NIH-PA Author Manuscript

NIH-PA Author Manuscript

26. Smith EL 3rd, Kee CS, Ramamirtham R, Qiao-Grider Y, Hung LF. Peripheral vision can influence eye growth and refractive development in infant monkeys. Invest Ophthalmol Vis Sci. 2005; 46:3965–3972. [PubMed: 16249469]
27. Smith EL 3rd, Ramamirtham R, Qiao-Grider Y, Hung LF, Huang J, Kee CS, Coats D, Paysse E. Effects of foveal ablation on emmetropization and form-deprivation myopia. Invest Ophthalmol Vis Sci. 2007; 48:3914–3922. [PubMed: 17724167]
28. Cho P, Cheung SW, Edwards M. The longitudinal orthokeratology research in children (LORIC) in Hong Kong: a pilot study on refractive changes and myopic control. Curr Eye Res. 2005; 30:71–80. [PubMed: 15875367]
29. Walline JJ, Jones LA, Sinnott LT. Corneal reshaping and myopia progression. Br J Ophthalmol. 2009; 93:1181–1185. [PubMed: 19416935]
30. Logan NS, Gilmartin B, Wildsoet CF, Dunne MC. Posterior retinal contour in adult human anisomyopia. Invest Ophthalmol Vis Sci. 2004; 45:2152–2162. [PubMed: 15223789]
31. Millodot M. Effect of ametropia on peripheral refraction. Am J Optom Physiol Opt. 1981; 58:691–695. [PubMed: 7294139]
32. Schmid GF. Axial and peripheral eye length measured with optical low coherence reflectometry. J Biomed Opt. 2003; 8:655–662. [PubMed: 14563204]
33. Atchison DA, Pritchard N, Schmid KL. Peripheral refraction along the horizontal and vertical visual fields in myopia. Vision Res. 2006; 46:1450–1458. [PubMed: 16356528]
34. Schmid GF. Variability of retinal steepness at the posterior pole in children 7–15 years of age. Curr Eye Res. 2003; 27:61–68. [PubMed: 12868010]
35. Hoogerheide J, Rempt F, Hoogenboom WP. Acquired myopia in young pilots. Ophthalmologica. 1971; 163:209–215. [PubMed: 5127164]
36. Mutti DO, Sholtz RI, Friedman NE, Zadnik K. Peripheral refraction and ocular shape in children. Invest Ophthalmol Vis Sci. 2000; 41:1022–1030. [PubMed: 10752937]
37. Schmid G. Retinal steepness vs. myopic shift in children. Optom Vis Sci. 2004; 81 Suppl.:81.
38. Mutti DO, Hayes JR, Mitchell GL, Jones LA, Moeschberger ML, Cotter SA, Kleinstein RN, Manny RE, Twelker JD, Zadnik K. Refractive error, axial length, and relative peripheral refractive error before and after the onset of myopia. Invest Ophthalmol Vis Sci. 2007; 48:2510–2519. [PubMed: 17525178]
39. Curcio CA, Sloan KR, Kalina RE, Hendrickson AE. Human photoreceptor topography. J Comp Neurol. 1990; 292:497–523. [PubMed: 2324310]
40. Horner DG, Soni PS, Salmon TO, Swartz TS. Myopia progression in adolescent wearers of soft contact lenses and spectacles. Optom Vis Sci. 1999; 76:474–479. [PubMed: 10445639]
41. Walline JJ, Jones LA, Sinnott L, Manny RE, Gaume A, Rah MJ, Chitkara M, Lyons S. A randomized trial of the effect of soft contact lenses on myopia progression in children. Invest Ophthalmol Vis Sci. 2008; 49:4702–4706. [PubMed: 18566461]
42. Marsh-Tootle WL, Dong LM, Hyman L, Gwiazda J, Weise KK, Dias L, Fern KD. Myopia progression in children wearing spectacles vs. switching to contact lenses. Optom Vis Sci. 2009; 86:741–747.
43. Perrigin J, Perrigin D, Quintero S, Grosvenor T. Silicone-acrylate contact lenses for myopia control: 3-year results. Optom Vis Sci. 1990; 67:764–769. [PubMed: 2247299]
44. Stone J. The possible influence of contact lenses on myopia. Br J Physiol Opt. 1976; 31:89–114. [PubMed: 1052437]
45. Katz J, Schein OD, Levy B, Cruiscullo T, Saw SM, Rajan U, Chan TK, Yew Khoo C, Chew SJ. A randomized trial of rigid gas permeable contact lenses to reduce progression of children's myopia. Am J Ophthalmol. 2003; 136:82–90. [PubMed: 12834674]
46. Baldwin WR, West D, Jolley J, Reid W. Effects of contact lenses on refractive corneal and axial length changes in young myopes. Am J Optom Arch Am Acad Optom. 1969; 46:903–911. [PubMed: 5262334]
47. Walline JJ, Jones LA, Mutti DO, Zadnik K. A randomized trial of the effects of rigid contact lenses on myopia progression. Arch Ophthalmol. 2004; 122:1760–1766. [PubMed: 15596577]

NIH-PA Author Manuscript

NIH-PA Author Manuscript

NIH-PA Author Manuscript

48. Atchison DA. Aberrations associated with rigid contact lenses. J Opt Soc Am (A). 1995; 12:2267–2273.
49. Cheng X, Himebaugh NL, Kollbaum PS, Thibos LN, Bradley A. Validation of a clinical Shack-Hartmann aberrometer. Optom Vis Sci. 2003; 80:587–595. [PubMed: 12917578]
50. Shen J, Thibos LN. Measuring ocular aberrations and image quality in peripheral vision with a clinical wavefront aberrometer. Clin Exp Optom. 2009; 92:212–222. [PubMed: 19462503]
51. Mathur A, Atchison DA, Kasthurirangan S, Dietz NA, Luong S, Chin SP, Lin WL, Hoo SW. The influence of oblique viewing on axial and peripheral refraction for emmetropes and myopes. Ophthalmic Physiol Opt. 2009; 29:155–161. [PubMed: 19236585]
52. Hom, MM. Rigid lens design and fitting. In: Hom, MM., editor. Manual of Contact Lines Prescribing and Fitting. Boston: Butterworth-Heinemann; 1997. p. 77-103.
53. Thibos LN, Wheeler W, Horner D. Power vectors: an application of Fourier analysis to the description and statistical analysis of refractive error. Optom Vis Sci. 1997; 74:367–375. [PubMed: 9255814]
54. Thibos LN, Hong X, Bradley A, Applegate RA. Accuracy and precision of objective refraction from wavefront aberrations. J Vis. 2004; 4:329–351. [PubMed: 15134480]
55. Ferree CE, Rand G, Hardy C. Refraction for the peripheral field of vision. Arch Ophthalmol. 1931; 5:717–731.
56. Atchison DA, Scott DH, Charman WN. Hartmann-Shack technique and refraction across the horizontal visual field. J Opt Soc Am (A). 2003; 20:965–973.
57. Rempt F, Hoogerheide J, Hoogenboom WP. Peripheral retinoscopy and the skiagram. Ophthalmologica. 1971; 162:1–10. [PubMed: 5547863]
58. Le Grand, Y. Form and Space Vision. revised ed. Millodot, M.; Heath, GG., translators. Bloomington, IN: Indiana University Press; 1967.
59. Lotmar W, Lotmar T. Peripheral astigmatism in the human eye: experimental data and theoretical model predictions. J Opt Soc Am. 1974; 64:510–513. [PubMed: 4822573]
60. Atchison DA. Optical models for human myopic eyes. Vision Res. 2006; 46:2236–2250. [PubMed: 16494919]
61. Atchison DA, Scott DH. Monochromatic aberrations of human eyes in the horizontal visual field. J Opt Soc Am (A). 2002; 19:2180–2184.
62. Navarro R, Moreno E, Dorronsoro C. Monochromatic aberrations and point-spread functions of the human eye across the visual field. J Opt Soc Am (A). 1998; 15:2522–2529.
63. Tabernero J, Schaeffel F. More irregular eye shape in low myopia than in emmetropia. Invest Ophthalmol Vis Sci. 2009; 50:4516–4522. [PubMed: 19474403]
64. Atchison DA, Jones CE, Schmid KL, Pritchard N, Pope JM, Strugnell WE, Riley RA. Eye shape in emmetropia and myopia. Invest Ophthalmol Vis Sci. 2004; 45:3380–3386. [PubMed: 15452039]
65. Siegel, S. Nonparametric Statistics for the Behavioral Sciences. New York: McGraw-Hill; 1956.
66. Wang YZ, Thibos LN. Oblique (off-axis) astigmatism of the reduced schematic eye with elliptical refracting surface. Optom Vis Sci. 1997; 74:557–562. [PubMed: 9293525]
67. Escudero-Sanz I, Navarro R. Off-axis aberrations of a wide-angle schematic eye model. J Opt Soc Am (A). 1999; 16:1881–1891.
68. Charman WN. Aberrations and myopia. Ophthalmic Physiol Opt. 2005; 25:285–301. [PubMed: 15953113]
69. Marcos S, Barbero S, Llorente L. The sources of optical aberrations in myopic eyes. Invest Ophthalmol Vis Sci. 2002; 43:E-Abstract 1510.
70. Thorn, F.; He, JC.; Thorn, SJ.; Held, R.; Gwiazda, J. The vision of myopic children: how wavefront aberrations alter the image of school book text. In: Thorn, F.; Troilo, D.; Gwiazda, J., editors. Myopia 2000: Proceedings of the VIII International Conference on Myopia; Boston: The New England College of Optometry; July 7–9, 2000; Boston, MA. 2000. p. 127-131.
71. Wildsoet, CF. Structural correlates of myopia. In: Gilmartin, B.; Rosenfirld, M., editors. Myopia and Nearwork. Boston: Butterworth-Heinemann; 1998. p. 31-56.

NIH-PA Author Manuscript

NIH-PA Author Manuscript

NIH-PA Author Manuscript

72. Kee CS, Hung LF, Qiao-Grider Y, Roorda A, Smith EL 3rd. Effects of optically imposed astigmatism on emmetropization in infant monkeys. Invest Ophthalmol Vis Sci. 2004; 45:1647–1659. [PubMed: 15161822]

73. Deller JF, O'Connor AD, Sorsby A. X-ray measurement of the diameters of the living eye. Proc R Soc Med. 1947; 134:456–467. [PubMed: 20265562]

74. Wang FR, Zhou XD, Zhou SZ. [A CT study of the relation between ocular axial biometry and refraction]. Zhonghua Yan Ke Za Zhi. 1994; 30:39–40. [PubMed: 8082473]

75. Bennett, AG.; Rabbetts, RB. Bennett and Rabbetts' Clinical Visual Optics. 3rd ed.. Boston: Butterworth Heinemann; 1998.

76. Artal P, Benito A, Tabernero J. The human eye is an example of robust optical design. J Vis. 2006; 6:1–7. [PubMed: 16489854]

77. Artal P, Guirao A, Berrio E, Williams DR. Compensation of corneal aberrations by the internal optics in the human eye. J Vis. 2001; 1:1–8. [PubMed: 12678609]

78. Fulton AB, Hansen RM, Petersen RA. The relation of myopia and astigmatism in developing eyes. Ophthalmology. 1982; 89:298–302. [PubMed: 7099549]

79. Irving EL, Callender MG, Sivak JG. Inducing ametropias in hatchling chicks by defocus—aperture effects and cylindrical lenses. Vision Res. 1995; 35:1165–1174. [PubMed: 7610578]

80. McLean RC, Wallman J. Severe astigmatic blur does not interfere with spectacle lens compensation. Invest Ophthalmol Vis Sci. 2003; 44:449–457. [PubMed: 12556368]

81. Schmid K, Wildsoet CF. Natural and imposed astigmatism and their relation to emmetropization in the chick. Exp Eye Res. 1997; 64:837–847. [PubMed: 9245915]

82. Thibos LN, Cheng X, Phillips J, Collins A. Optical aberrations of chick eyes. Invest Ophthalmol Vis Sci. 2001; 43 E-Abstract 180.

83. Thibos LN, Cheng X, Phillips J, Collins A. Astigmatic deprivation of chicks produces myopia, but not astigmatism. Invest Ophthalmol Vis Sci. 2001; 42:S58.

NIH-PA Author Manuscript

NIH-PA Author Manuscript

NIH-PA Author Manuscript

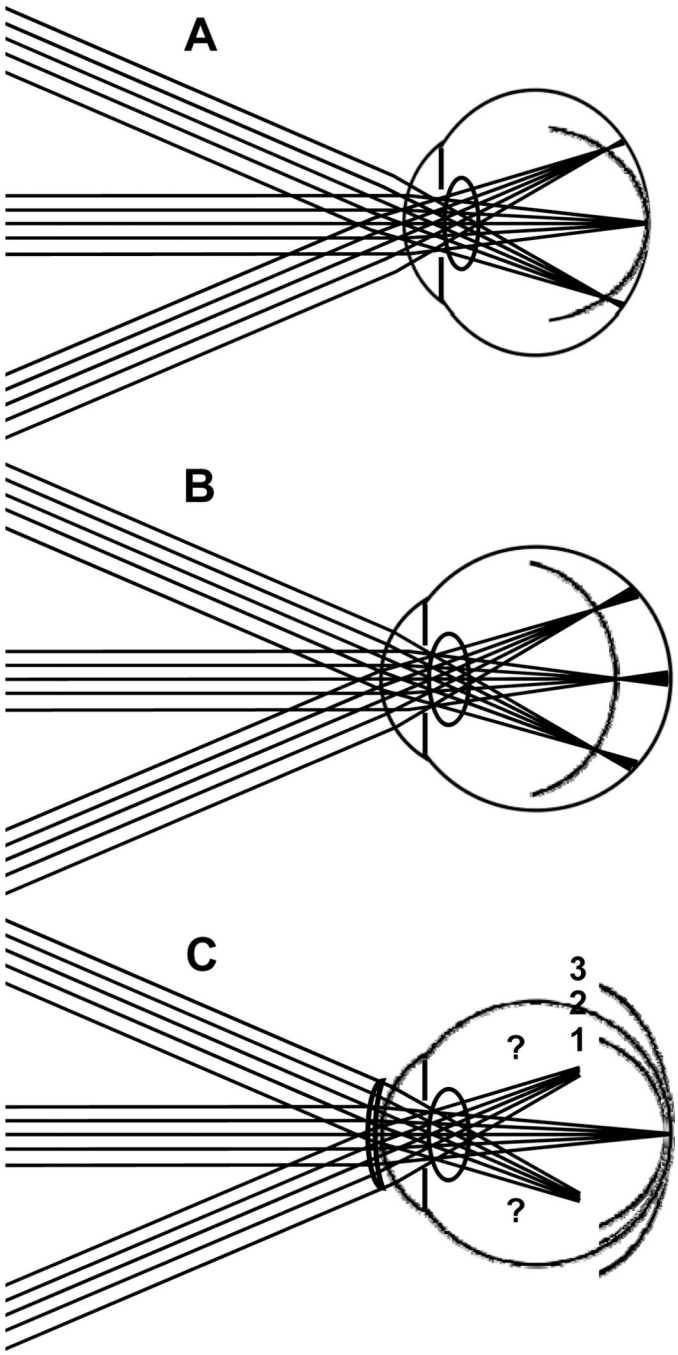

Figure 1.
Image shell formed in **(A)** emmetrope, **(B)** axial myopic eye and **(C)** contact lens corrected myopic eye. Parts **(A)** and **(B)** summarize conceptually the relationship between the image shell formed by the eye's optical system and the retinal profile as reported in the literature. Part C shows potential effects on the image shell of contact lens correction of foveal refractive error. We report the combined effects of retinal profile and optics as measured by refractive error across the visual field.

NIH-PA Author Manuscript

NIH-PA Author Manuscript

NIH-PA Author Manuscript

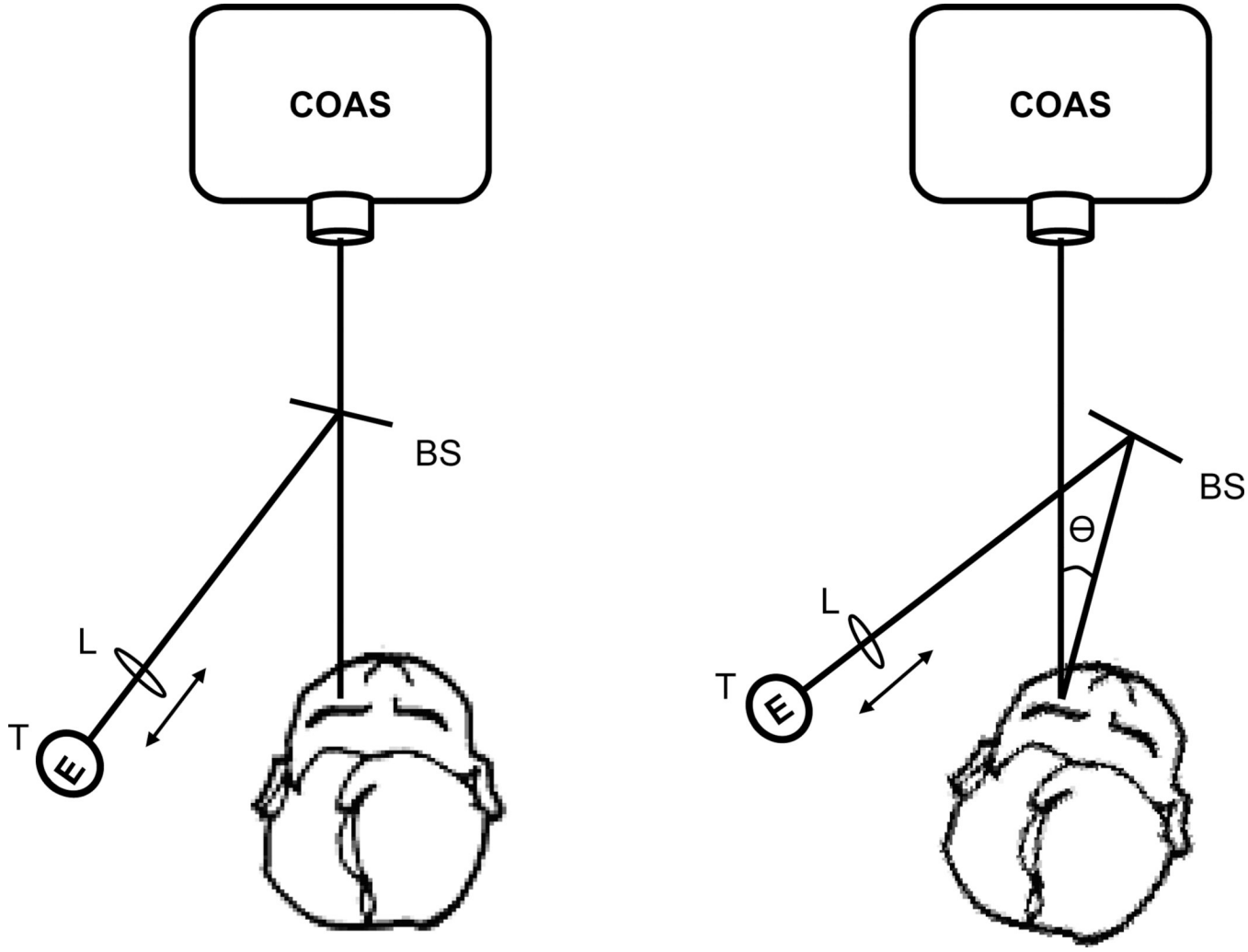

Figure 2.
Instrument setup: chin rest was modified to be able to rotate in the horizontal meridian by angle θ and a fixation target (T) was rendered visible to the subject through a beam splitter (BS). The vergence of the target was adjusted by axial displacement of lens (L). T, BS and L were all attached to the chin rest so they rotated as a unit with the chin rest. The fixation target coincided with the laser probe beam of the aberrometer when the head was in the straight-ahead position.

NIH-PA Author Manuscript
NIH-PA Author Manuscript
NIH-PA Author Manuscript

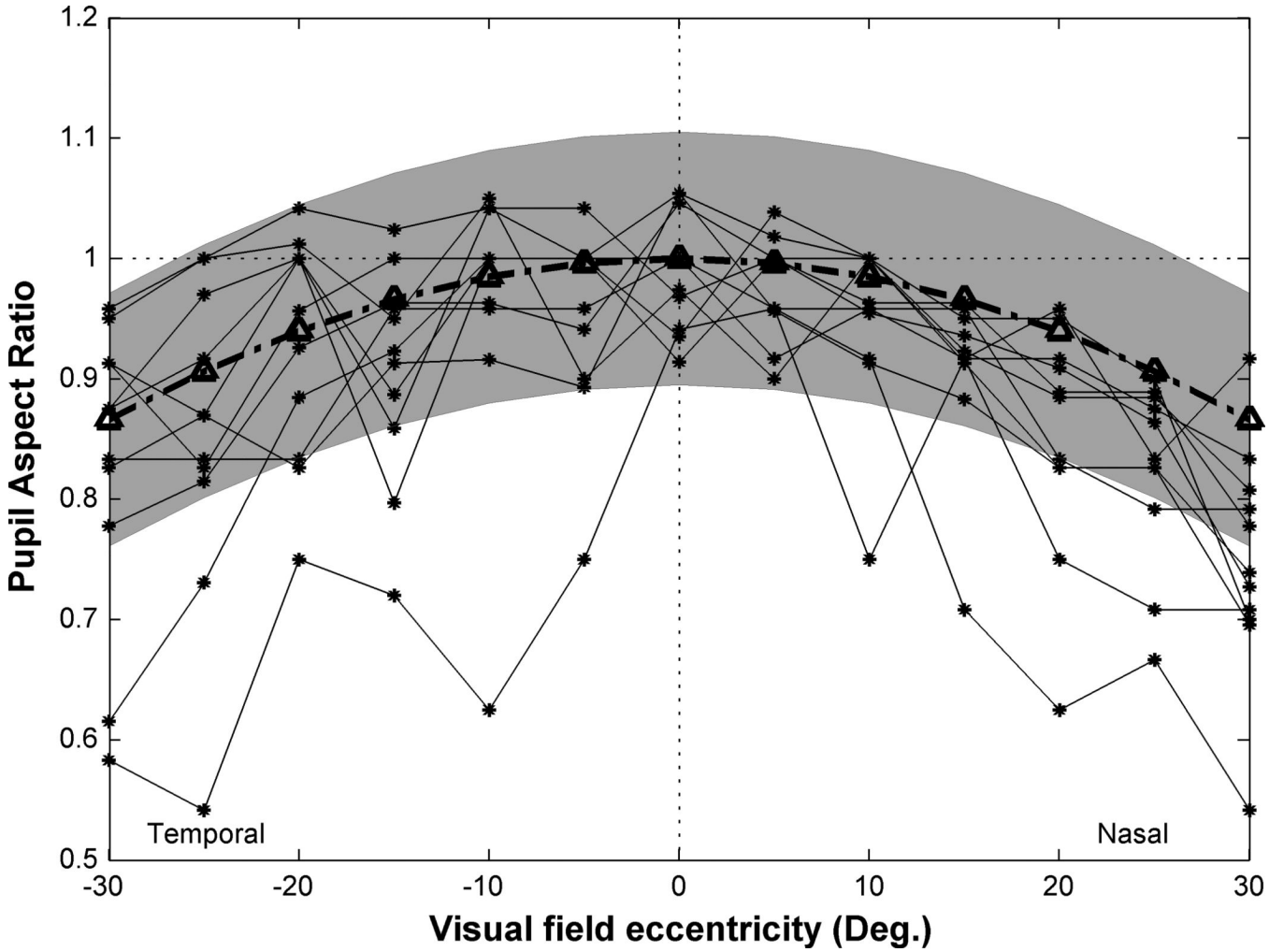

Figure 3.

The range of eccentricities (relative to the foveal line-of-sight) accessible in human subjects. Y axis is pupil aspect ratio which defined as entrance pupil diameter in horizontal meridian divided by entrance pupil diameter in vertical meridian. The broken line with triangle symbol indicates the theoretical prediction of this ratio by cosine law. Shaded zone indicates a range of acceptable values equal to (number of raw spots in horizontal meridian ±1 / number of raw spots in vertical meridian ±1). The black lines connecting asterisk symbols indicate the actual pupil aspect ratio estimated from the number of illuminated lenslets for each subject.

NIH-PA Author Manuscript
NIH-PA Author Manuscript
NIH-PA Author Manuscript

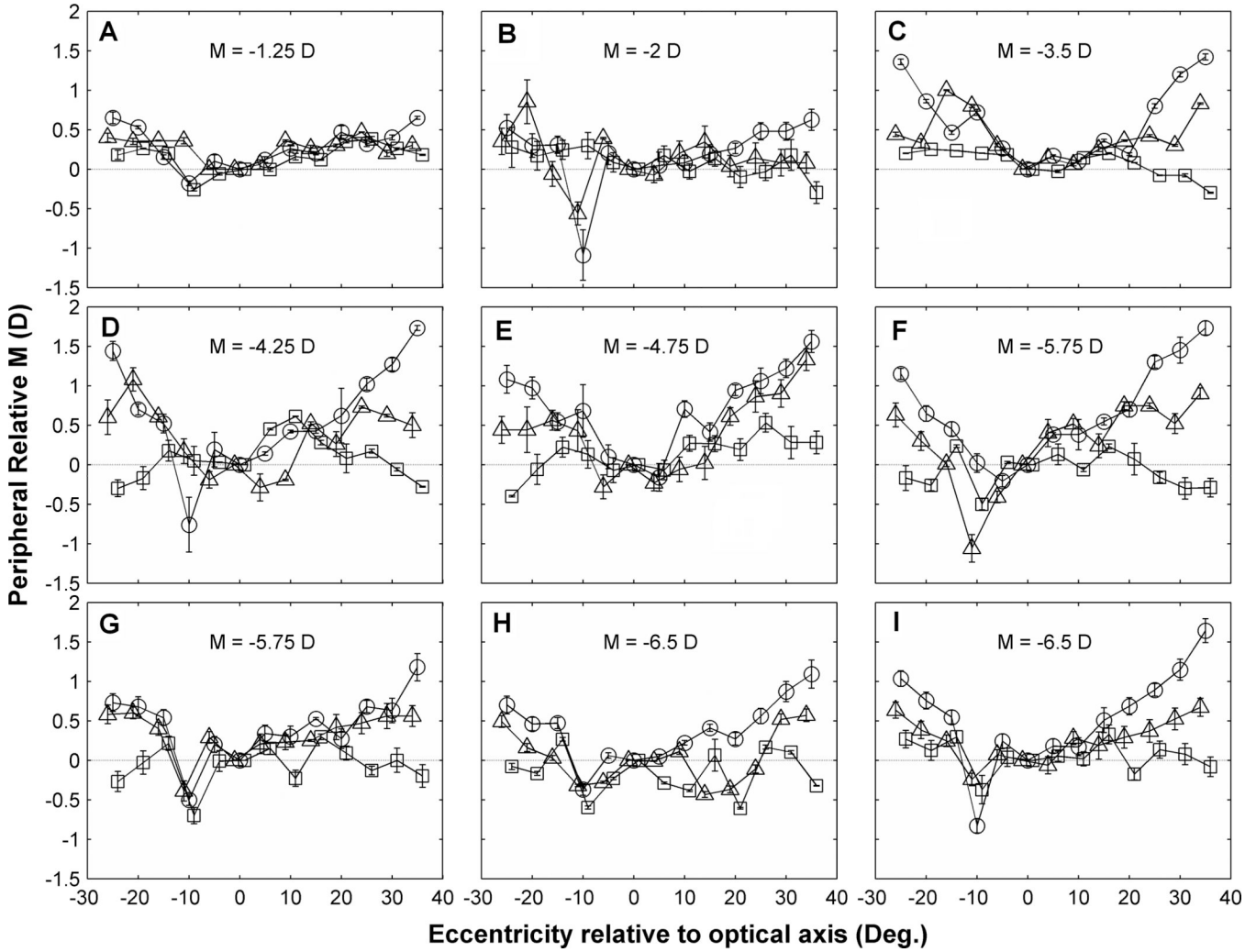

Figure 4.

PRM variations across horizontal visual field in 9 individual eyes **(A ~ I)** with and without contact lens correction. X axis is the eccentricity relative to optical axis (which is temporal 5° relative to foveal LoS). Y axis is the relative M which is equal to (peripheral M – M on the optical axis). Symbols indicate PRM in the naked eye (circles), in eyes corrected with SCLs (triangles), and in eyes corrected with RGP lenses (squares). Error bars show the standard error of the mean (SEM) of averaged PRM for 3 measurements at each eccentricity. Axial myopia M of each eye is indicated on each panel. For clarity, symbols and error bars are slightly staggered horizontally. Visual field eccentricities are referenced to the optical axis (see Methods) to remove nasal/temporal asymmetries from the data.

NIH-PA Author Manuscript
NIH-PA Author Manuscript
NIH-PA Author Manuscript

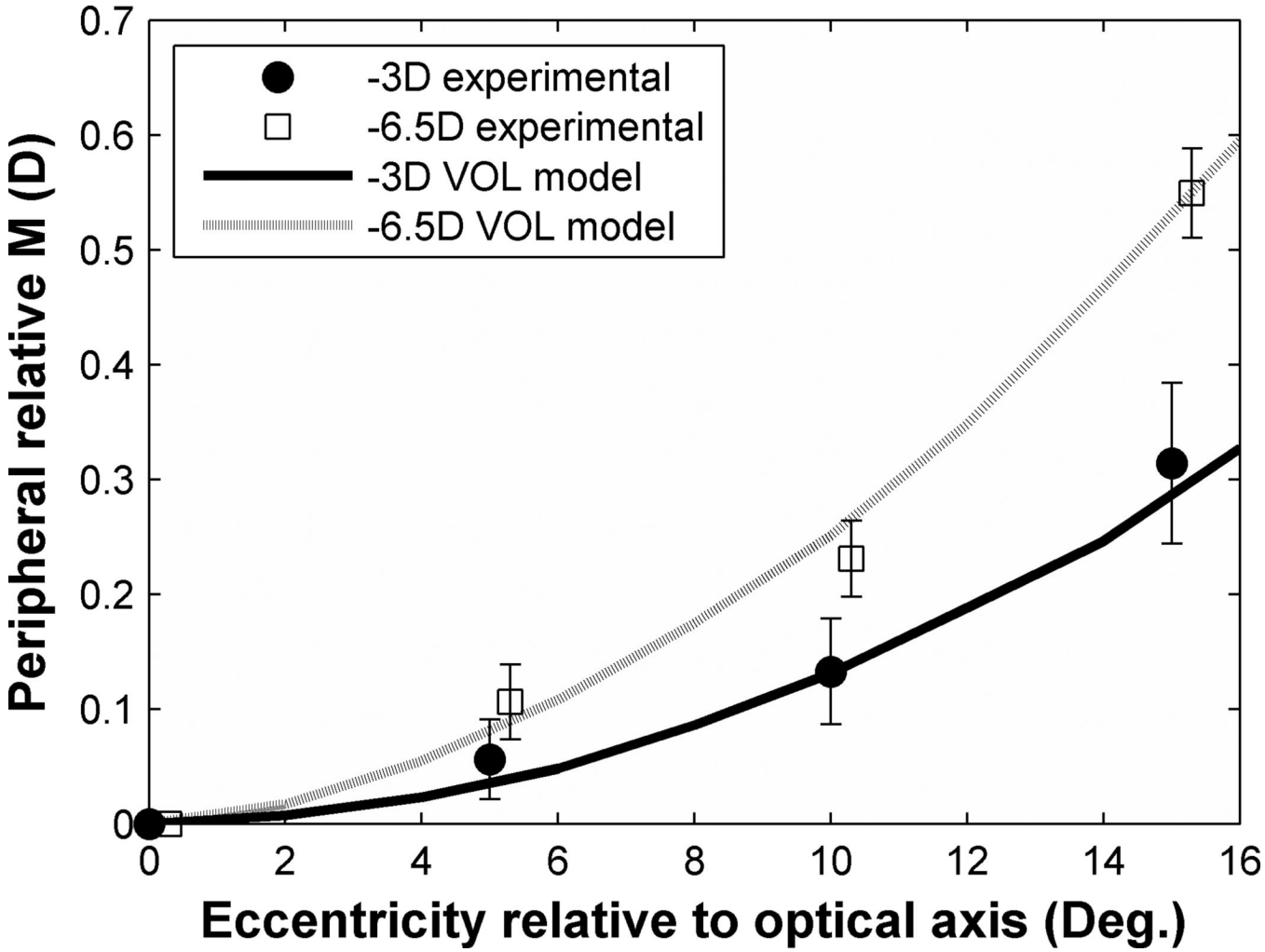

Figure 5.

Optical prediction and experimental data of the change of PRM with increased off-axis viewing. X axis refers to eccentricities relative to the optical axis. Dotted and solid curves indicate predicted values of PRM from VOL calculation with visual field eccentricities increasing. Filled circle symbols indicate the experimental data of −2D myopic eye and open square symbols indicate the experimental data of −6.5D myopic eye. Error bars indicate the standard error of the mean (SEM) in each set of measurements. For clarity, symbols and error bars are slightly staggered horizontally.

NIH-PA Author Manuscript

NIH-PA Author Manuscript

NIH-PA Author Manuscript

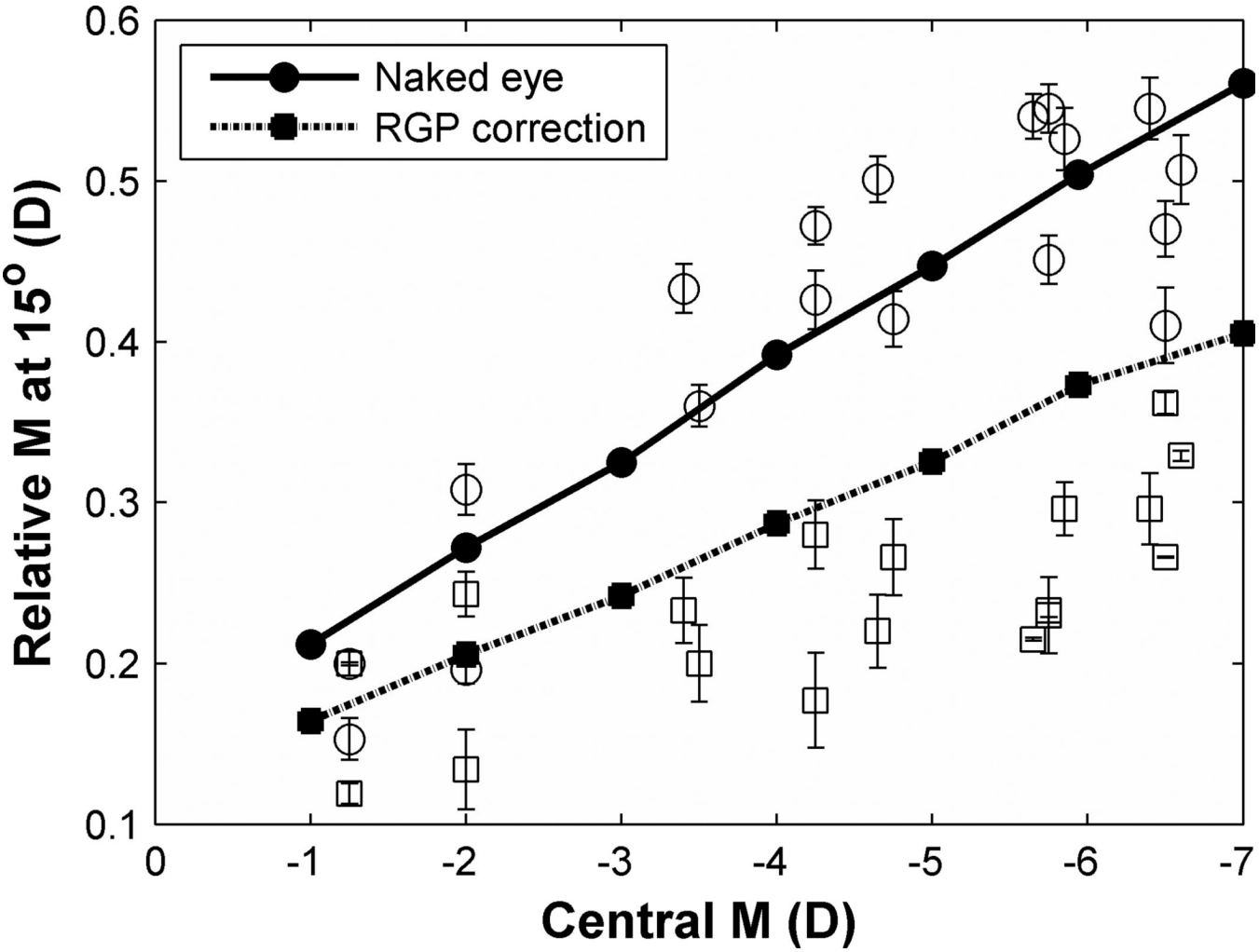

Figure 6.

Changes of peripheral relative spherical equivalent as a function of central spherical equivalent (M). Y axis is relative M at 15° field angle, relative to optical axis, computed as peripheral M – central M. Solid and dash lines are the theoretical predictions of PRM as functions of central M in naked eyes and PRG corrected eyes calculated from VOL using Atchison's myopic model eye. Circles and squares represent experimental data in naked eyes and RGP corrected eyes, respectively, at 15° in both visual fields. Error bars indicate SEM of the three measurements for each subject.

NIH-PA Author Manuscript
NIH-PA Author Manuscript
NIH-PA Author Manuscript

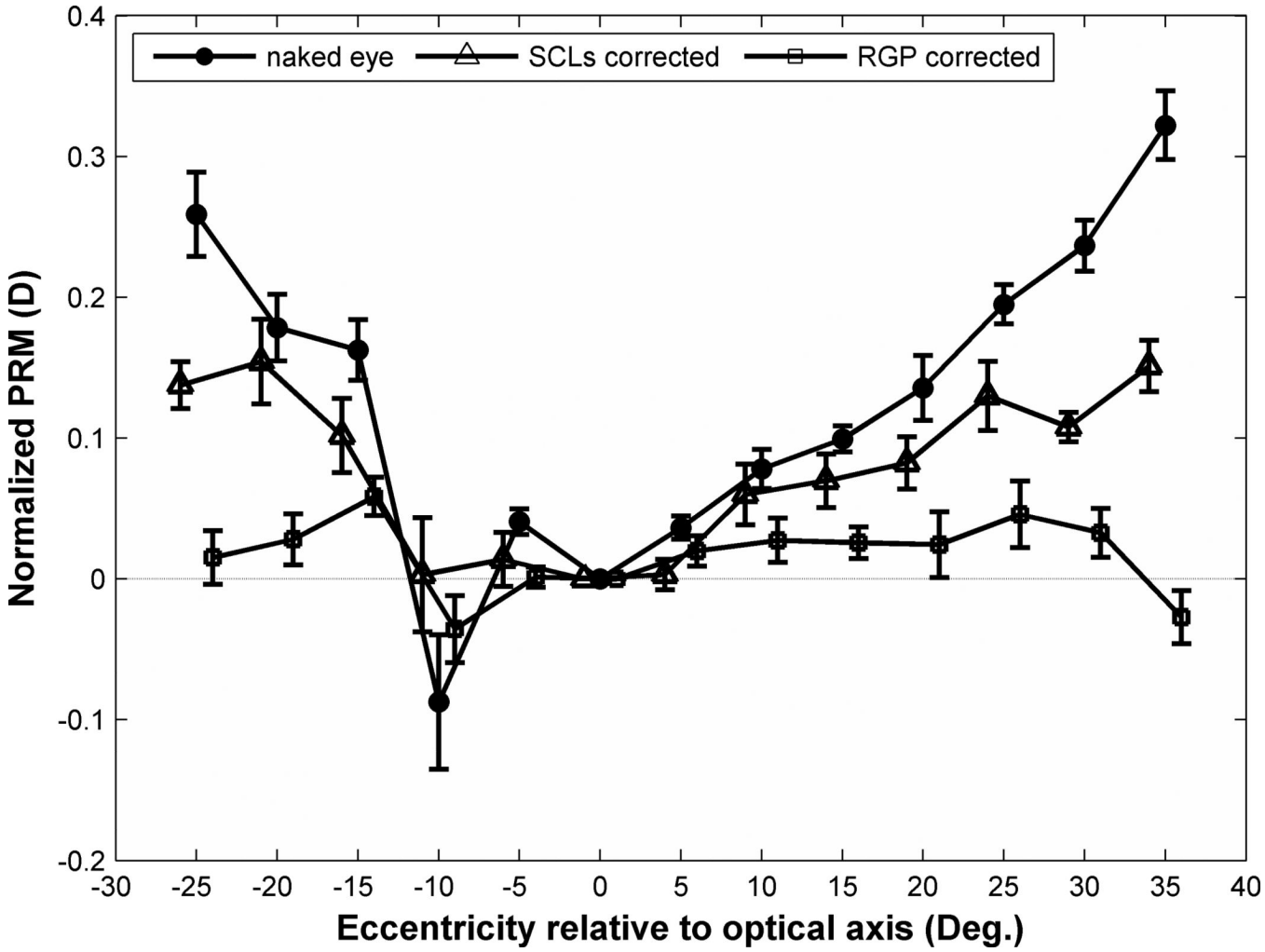

Figure 7.

Effect of eccentricity on normalized PRM before and after contact lens correction. Symbols indicate population means of normalized PRM in the naked eye (filled circles), in eyes corrected with SCLs (triangles), and in eyes corrected with RGP lenses (squares). Error bar shows the standard error of the mean (SEM) of normalized PRM for the test population of 9 subjects. For clarity, symbols and error bars are slightly staggered horizontally.

NIH-PA Author Manuscript
NIH-PA Author Manuscript
NIH-PA Author Manuscript

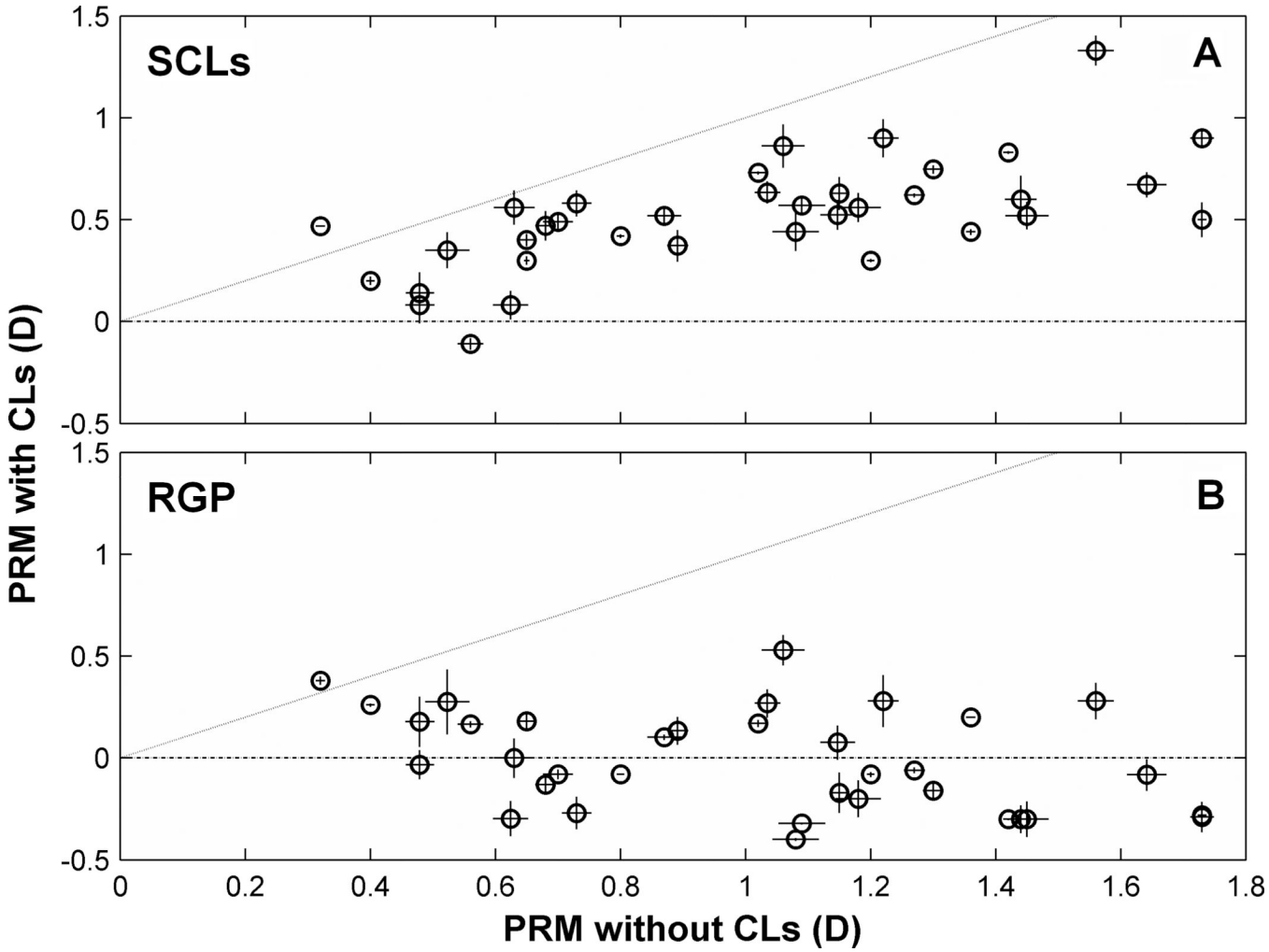

Figure 8.

Effect of SCLs **(A)** and RGP **(B)** lenses on PRM. Both X and Y axes indicate as peripheral relative spherical equivalent defined by (peripheral M – central M). Negative axes value means a relatively myopic periphery and positive axes value means a relatively hyperopic periphery. One to one dotted lines indicate a situation that PRM are exactly same before and after CLs correction. Each data point here represents a mean value of three measurements at the largest eccentricity measured (25°–30°). Error bars of each data point in horizontal and vertical meridian indicate SEM of the three measurements taken without contact lens and with contact lens, respectively.

NIH-PA Author Manuscript
NIH-PA Author Manuscript
NIH-PA Author Manuscript

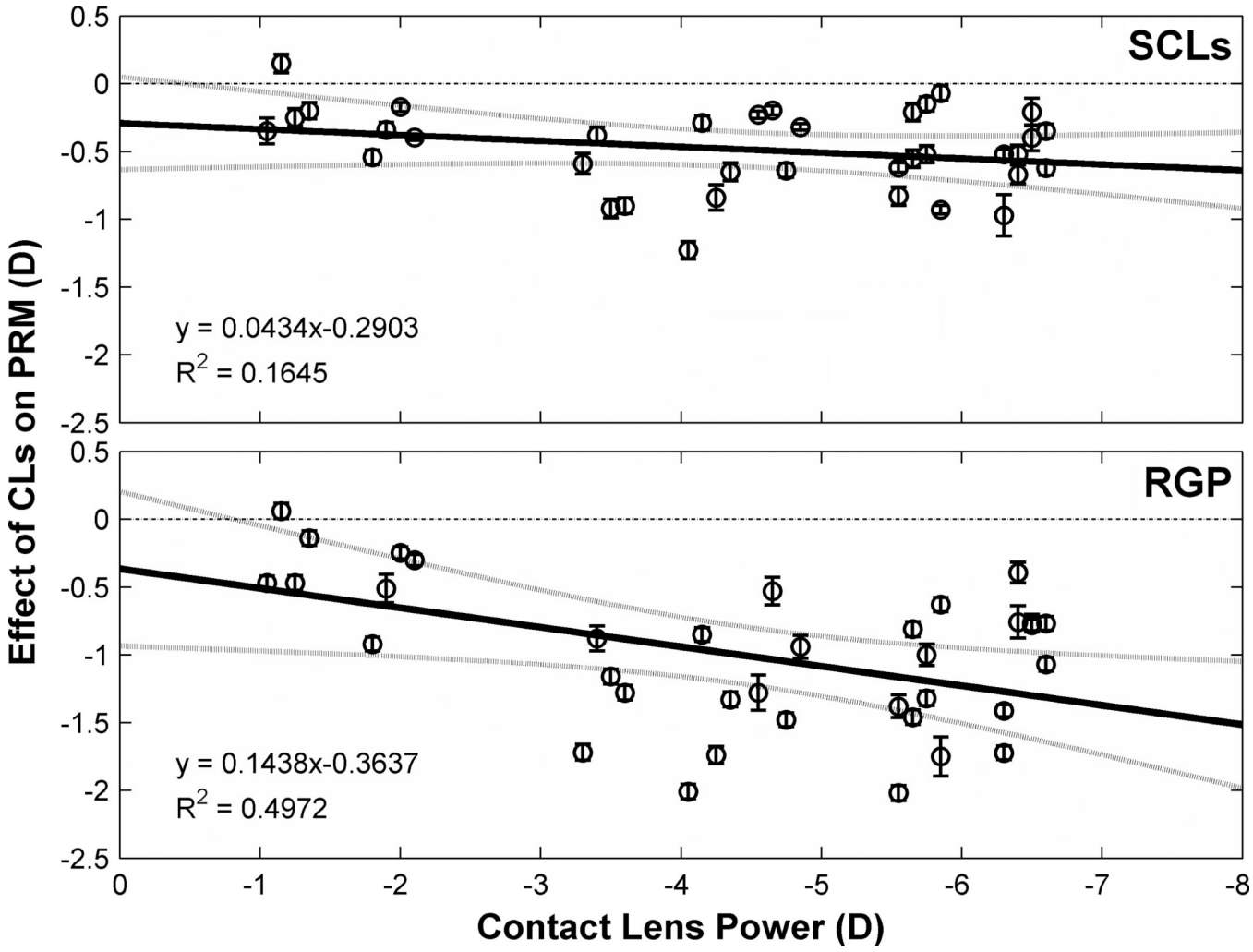

Figure 9.

Effect of CLs on PRM as a function of CLs power. Y axis indicates the effect of CLs, computed as (PRM with CLs correction – PRM without CLs correction). Data points represent mean value of three measurements at each visual field eccentricities for a given eye. The y=0 dashed lines is the prediction if CLs with variant powers have no effect on PRM. Solid lines are orthogonal regression lines fitted on the data points and dotted curves show 95% confidence interval of these regression lines. Error bars are SEM of the three measurements in a certain visual angle. For clarity, symbols and error bars are slightly staggered horizontally.

NIH-PA Author Manuscript
NIH-PA Author Manuscript
NIH-PA Author Manuscript

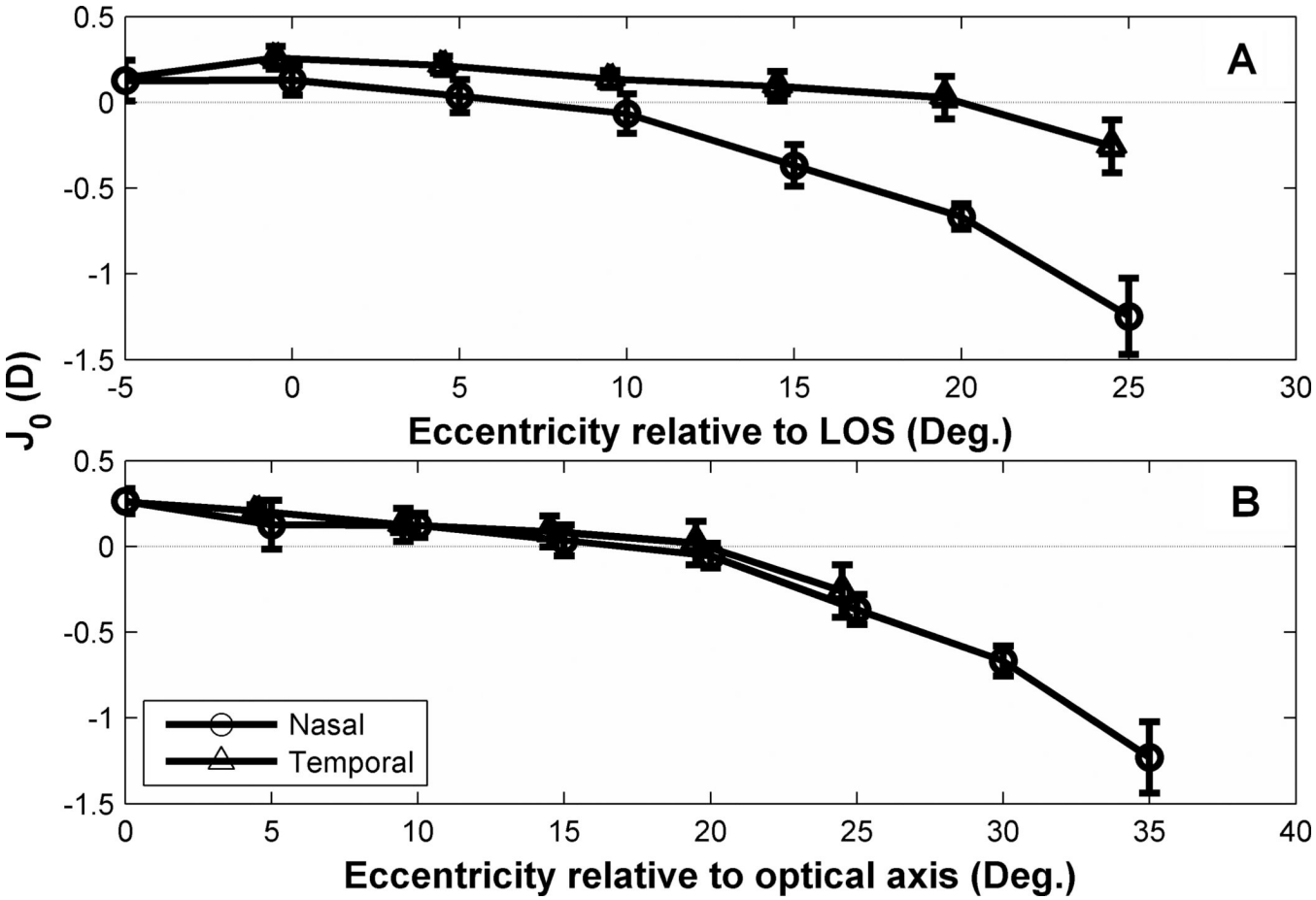

Figure 10.

Changes of mean J_0 as a function of visual field eccentricities in the uncorrected eye. Data points are the mean value of J_0 for all subjects. Error bars indicate SEM of J_0 for all nine subjects. Note: **(A)** and **(B)** have different×axis label. X axis in **(A)** is visual field angle relative to the foveal line-of-sight (LoS). X axis in **(B)** refers to eccentricities relative to the optical axis (temporal 5° in A). For example, 10° in **(B)** corresponds to 5° in nasal visual field and 15° in temporal visual field in (A). For clarity, symbols and error bars are slightly staggered horizontally.

NIH-PA Author Manuscript
NIH-PA Author Manuscript
NIH-PA Author Manuscript

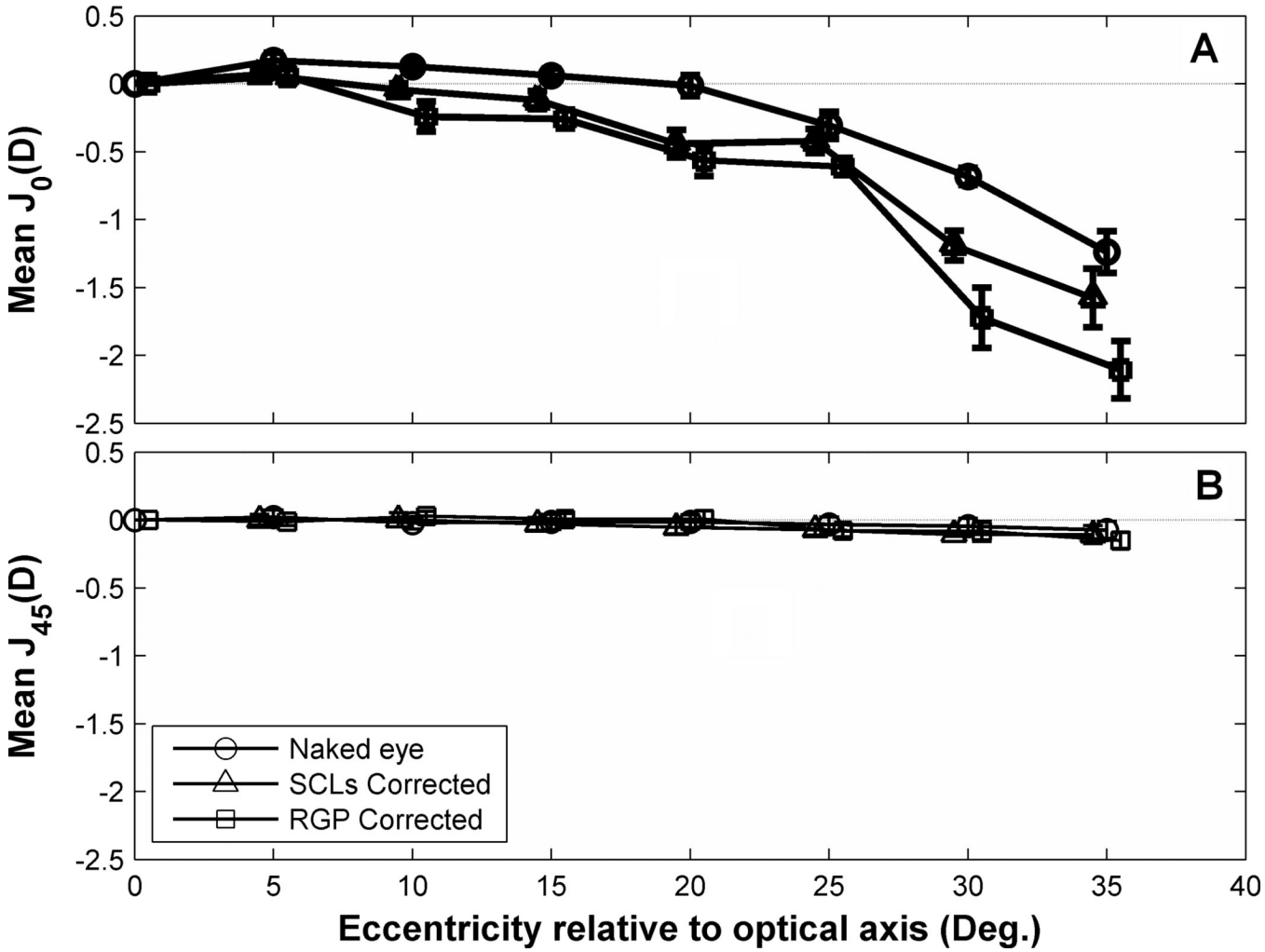

Figure 11.

Peripheral relative astigmatism before and after contact lens correction. **(A)** Mean PRJ_0 and **(B)** mean PRJ_{45} change as a function of eccentricity relative to optical axis. Error bars indicate SEM of the PRJ_0 and PRJ_{45} for all subjects. Symbols and error bars are slightly staggered horizontally for clarity.

NIH-PA Author Manuscript

NIH-PA Author Manuscript

NIH-PA Author Manuscript

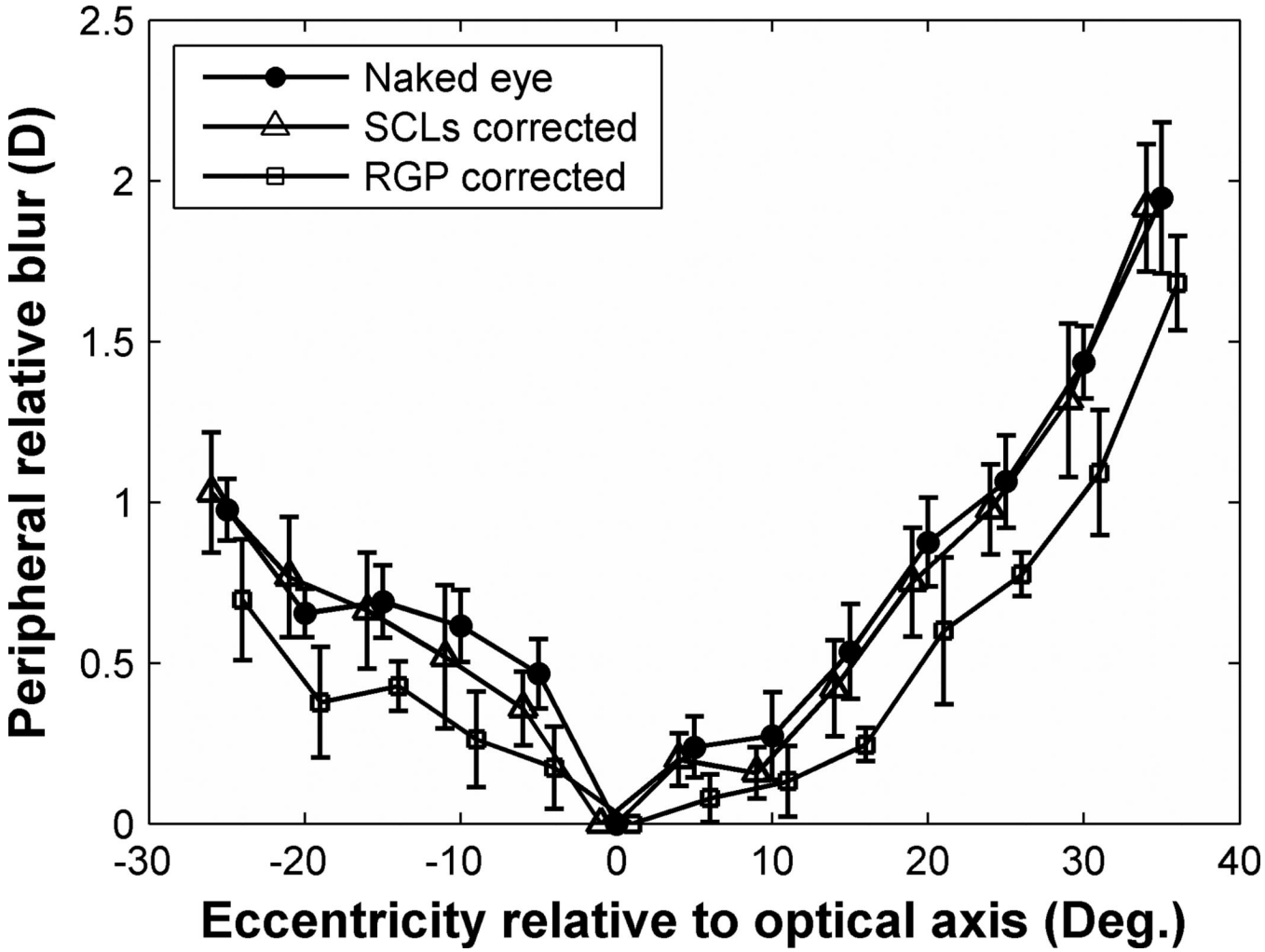

Figure 12.

Peripheral relative blur on the retina due to sphero-cylindrical refractive errors across the visual field relative to optical axis. Filled circle symbols represent population mean of PRBlur in naked eyes. Open triangle and square symbols represent data of SCLs correction and RGP correction, respectively. Error bars indicate SEM of the average PRBlur for all the subjects. For clarity, symbols and error bars are slightly staggered horizontally.

NIH-PA Author Manuscript

NIH-PA Author Manuscript

NIH-PA Author Manuscript

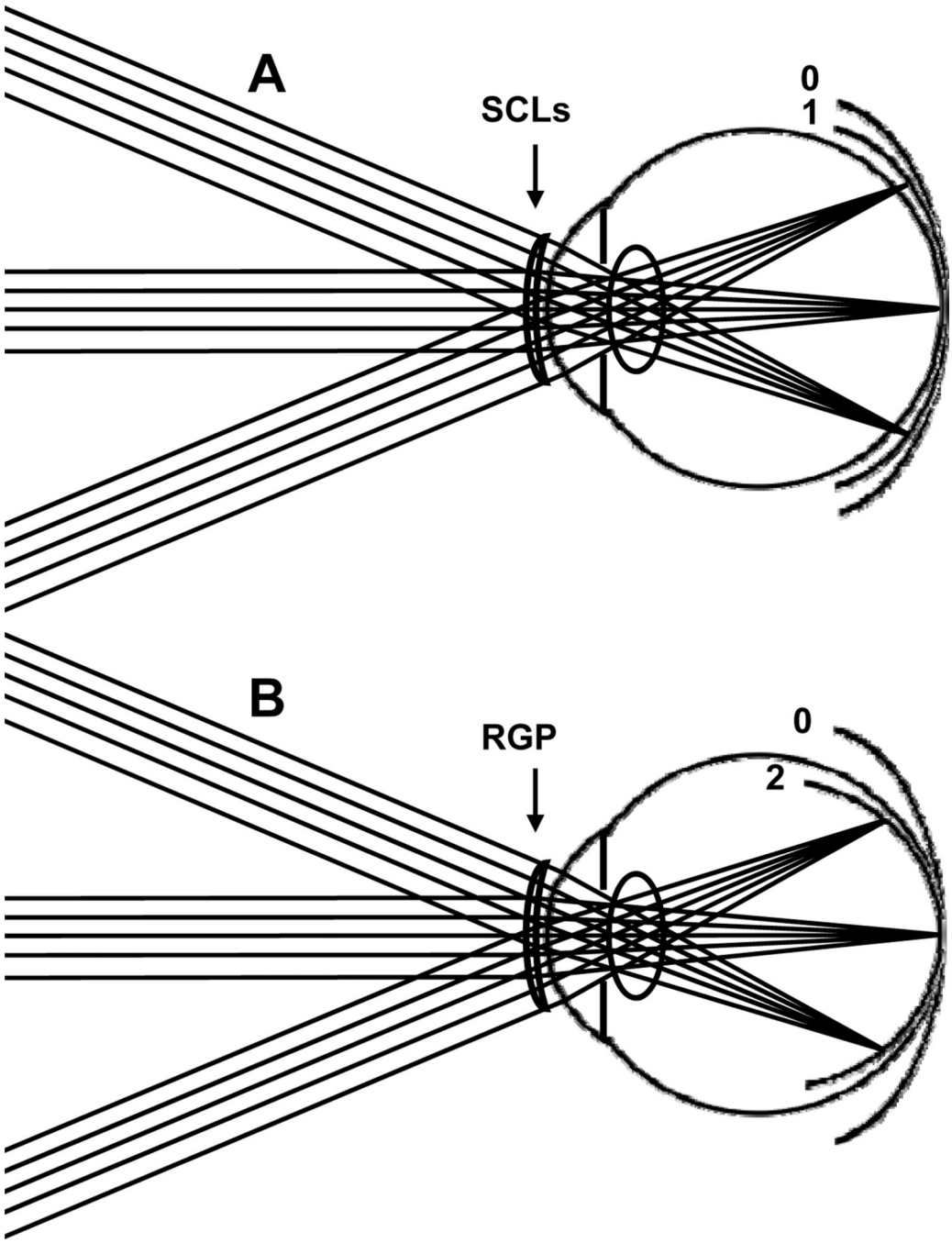

Figure 13.

Image shell formed with SCLs **(A)** or with RGP lens **(B)** correction in axially elongated myopic eye. Image shell #0 indicates a speculation that contact lenses have a constant power for all lines-of-sight, there would be no change in the hyperopic curvature of field. Image shell #1 and #2 illustrate the possible forms of peripheral field curvature after SCLs and RGP lens correction. The positions of these image shells are schematic only and do not represent a quantitative fit to our data.

NIH-PA Author Manuscript

NIH-PA Author Manuscript

NIH-PA Author Manuscript

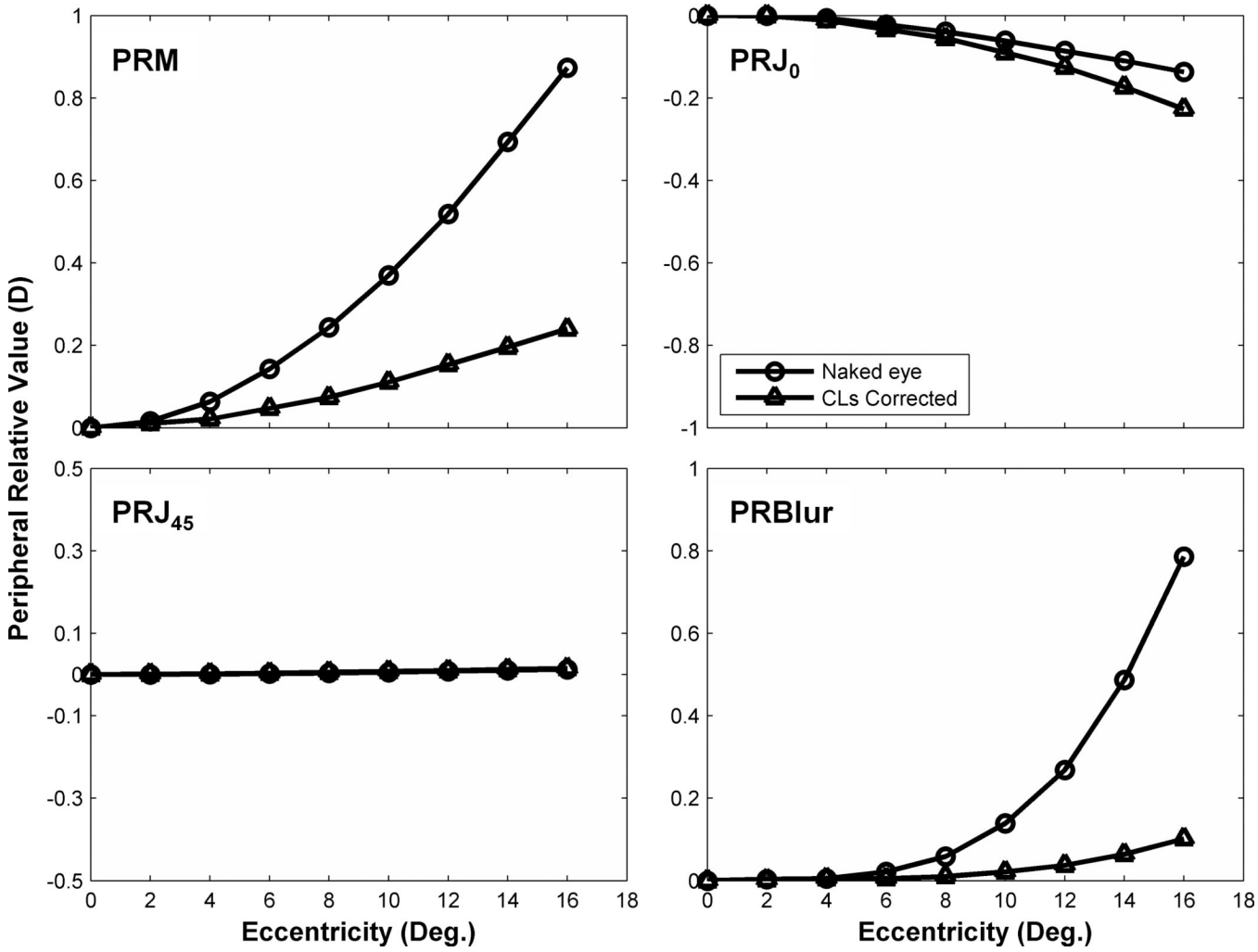

Figure 14.

VOL predictions of PRM, PRJ_0, PRJ_{45} and PRBlur changes as a function of off-axis eccentricity with and without contact lens correction. Circles indicate the prediction in the naked eye and open triangles indicate the predicted value with CLs correction.